UNIVERSITAT POLITÈCNICA DE CATALUNYA
BARCELONATECH
Escola d'Enginyeria de Barcelona Est

TREBALL FI DE MÀSTER

Màster en Ciència i Enginyeria de Materials / EEIGM

EFFECT OF LOADING AND RELEASE FACTORS *IN VITRO* OF MESOPOROUS SILICA NANOPARTICLES AS DRUG CARRIERS FOR NIFEDIPINE.

Memòria i Annexos

Autor: Lorène Galmiche
Director: José María MANERO

Convocatòria: Febrero 2018

Abstract

This project is a part of the development of biomaterials for bone tissue engineering for type 2 diabetic patients. The latters show a higher rejection implant rate than healthy people.

When people are affected by type 2 diabetes they develop insulin resistance and the glucose accumulates in blood. Hyperglycemia leads to the ROS (reactive oxygen species) production. The ROS takes part of an equilibrium (redox biology). They are used by cells in several mechanisms such as signal transduction, cellular proliferation or differentiation and development. However if they are overproduced, they become cytotoxic and leads to oxidative stress.
ROS have an impact on bone remodeling and enhance the resorption of bones. In the case of implant, a local treatment of ROS is needed to help the bone to form around the implant. To counterbalance the oxidative stress from the ROS, the nifedipine will be used for its anti-oxidative properties. But this drug is light sensitive and poorly soluble in water and it affects its bioavailability. To protect it and have a local treatment, silica mesoporous nanoparticles are used. Thanks to their high surface area and their high pore volume, it is possible to load a large quantity of drug inside the pores via adsorption. And the nanoparticles can bring a protection to the drug.

The aims of the project is to chose the best way to load nanoparticles among different methods and to choose a release method between three ones.

The first step of this project has been the synthesis of nanoparticles. The technique used is a sol-gel process where silica is obtained by the hydrolysis of TEOS on CTAB in a basic medium. A co-condensation was driven with APTES, the functionalization.

The second step was the loading of the nanoparticles with nifedipine. Four methods have been studied. The characterization has been done by Fourier transform infrared spectroscopy (FTIR) and thermogravimetric analysis (TGA). The FTIR gives evidence of the presence of nifedipine and the TGA allows to quantify it. The results show different percentage of loading which depend on the method used.

The third step was to study the release of nifedipine. Three different methods have been used: dialysis, USP apparatus and tubes. The characterization of the release has been processed by UV-vis NIR spectrophotometry at 238 nm. The three methods show a release of the drug but one is preferred.

Acknowledgments

I would like to thank warmly the whole group, BBT (Biomateriales, Biomecánica e Ingeniería de Tejidos) for having given me the possibility to do this internship.

I thank profusely José María Manero and Angélica Santos for their constant help during my project and for their availability.

I would like to thank also Carles Mas Moruno, Cristina Canal, Montse Espanol and Meritxell Molmeneu for their explications and their technical help.

I would like to thank Trifon Todorov, Montse Domínguez and Lluís Soler for their help during the measuring part.

Finally, I thank all the personal from the BBT group for its help and its daily kindness.

Glossary

Name	Abbreviation
Cetyltrimethylammonium bromide	CTAB
Tetraethyl orthosilicate	TEOS
(3-Aminopropyl)triethoxysilane	APTES
Nifedipine	Nif
Mesoporous silica nanoparticles functionalized with 2 mL of APTES	MSN-2-NH2
Mesoporous silica nanoparticles functionalized with 2 mL of APTES loaded with Nifedipine	MSN-2-NH2-Nif

Table of content

ABSTRACT I

ACKNOWLEDGMENTS III

GLOSSARY V

1. STATE OF THE ART 1

1. Type 2 Diabetes 1
   1) What is type 2 diabetes? 1
   2) Glucose toxicity 3
2. Reactive Oxygen Species 4
   1) What are they? 4
   2) The ROS take part of an equilibrium. 6
3. Bone disorder under diabetic mellitus 8
4. Nifedipine 10
   1) Properties 10
   2) Medicine 14
5. Nanoparticles 18
   1) Synthesis 18
   2) Drug loading and release study 22

2. AIMS OF THE PROJECT 24

3. MATERIALS AND METHODS 25

3.1. Synthesis 25
3.2. Purification 26
3.3. Loading 26
3.4. Release 32
   3.4.1. Dialysis 32
   3.4.1. USP apparatus 34
   3.4.2. Tubes 34
3.5. Baseline test 35
3.6. Characterization 35
   3.6.1. FTIR 35
   3.6.1. TGA 36
   3.6.2. UV-vis spectroscopy 37

4. RESULTS AND DISCUSSION 40

4.1. Purification 40
4.1.1. FTIR 40
4.2. Loading 41
4.2.1. FTIR 41
4.2.2 TGA 42
4.3. Release 44
4.3.1. UV-vis Spectroscopy 44

5. CONCLUSION 50

6. FURTHER WORK 52

7. ECONOMIC ANALYSIS 53

8. ENVIRONMENTAL IMPACT 56

9. ANNEXES 57

9.1. Annex A 57
9.2. Annex B 60
9.3. Annex C 61

10. BIBLIOGRAPHY 63

1. State of the art

This project is a part of the development of biomaterials for bone tissue engineering for type 2 diabetic patients. These latter show a higher rejection implant rate than healthy people. The aim is to bring a local treatment , in the border of the implant, to help the oragnism to accept the implant.

1. Type 2 Diabetes

1) What is type 2 diabetes?

The type 2 diabetes is the most present form of diabetes (about 90%). Most of the time it appears when people are adults (40-year-old and more). Unfortunately, more and more young people, even children, are affected by type 2 diabetes [1]. An OMS study shows that in 2014, 422 million of people were living with diabetes [2].

Diabetes is a chronical disease which implicates insulin resistance and a case of obesity most of the time.

In healthy people, all cells work with glucose. It is obtained by food or given by liver (out of meals during the night, for example). The glucose is driven to cells by way of blood. To penetrate cells, glucose needs help of a hormone which is produced by the beta cells in the pancreas: the insulin. The hormone attaches to the cell receptor which opens the gate, lets enter the glucose into the cell and leads to a decrease of glycemia (figure 1).

In diabetic people, at the beginning of the disease, the insulin secretion by beta cells is normal. But the obesity state stimulates cells to take energy from fatty acids and no more from glucose, causing a resistance to insulin of the cells (figure 1).
Therefore pancreatic islet cells produce more insulin to force cells to take it. With time the pancreatic cells have run through insulin, its production decreases then disappears and the glucose rate becomes abnormally high (hyperglycemia).

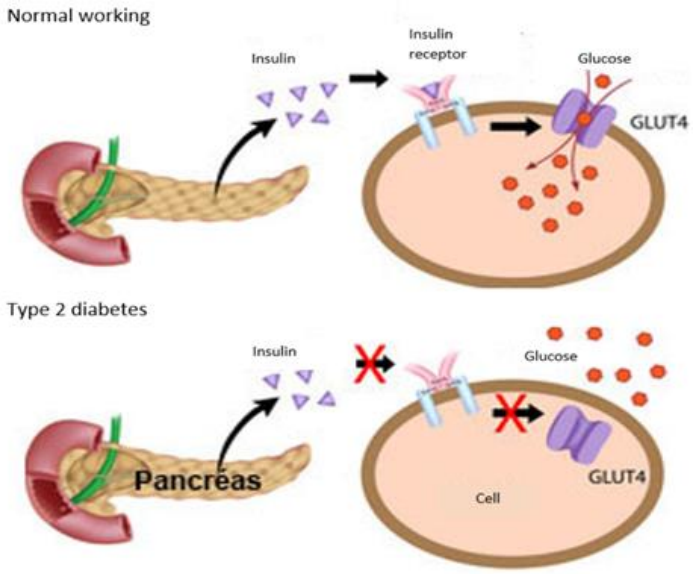

Figure 1 Scheme of insulin and glucose intercations in normal working and in type 2 diabetes. [3]

The type 2 diabetes, afterwards, can lead to complications such as skin infections, diabetic retinopathy, arteriosclerosis, heart damage, fatty liver, permanent kidney damage and osteoporosis (figure 2).

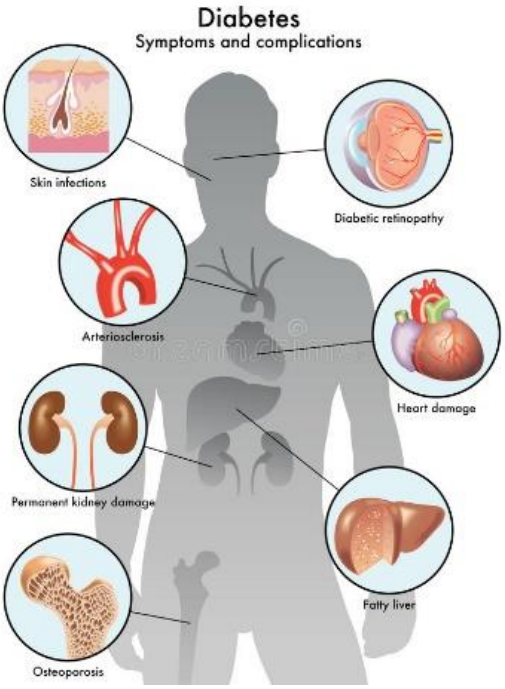

Figure 2 Diabetes complications. [3]

In the case of an implantation, the osteoporosis could give rise to difficulties in the osteointegration of the implant.

2) Glucose toxicity

A chronic hyperglycemia, due to diabetes, affects all tissues [1] and targets different organs which leads to different secondary dysfunctions such as retinopathy, kidney failure, neuropathies or macrovascular diseases and more particularly to the cells apoptosis and necrosis [4]. Indeed glucose in excess causes toxic effects on organs.

Different ways of this toxicity have in common the production of Reactive Oxygen Species (ROS) which cause oxidative stress and thus cell damage [5]. It has been proven that stable or intermittent high glucose level enhances oxidative stress generation [4]. A high oscillating glucose level is even more dangerous than a stable one. The antioxidative response of the cell is jeopardized, oxidative stress is increased which leads to cell apoptosis [4].
Several ways have been reported to develop ROS from glucose (figure 3) [5].

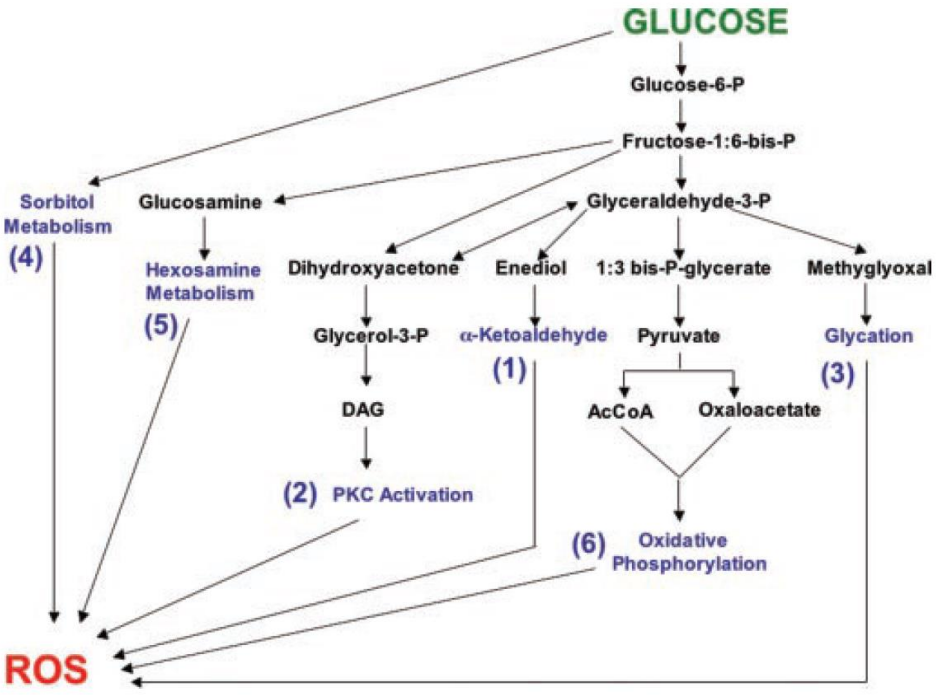

Figure 3 Different pathways from glucose to ROS.[5]

Pathway 1: enolization and α-ketoaldehyde formation. In the presence of redox active metals, H_2O_2 can form the toxic hydroxyl radical (it causes mutagenic alterations in DNA).
Pathway 2: PKC activation. It has biochemical consequences such as microvascular diseases in diabetes.
Pathway 3: dicarbonyl formation and glycation.

Pathway 4: sorbitol metabolism
Pathway 5: hexosamine metabolism. It is implicated in insulin resistance and in the rise of hydrogen peroxide levels.
Pathway 6: oxidative phosphorylation. It increases the superoxide production by a stimulation of mitochondrial activity.

Here, it is easily understandable that the increase of glucose leads to the rise of ROS.

The oxidative stress impairs beta cells function as well. The glucotoxicity has an influence on the insulin gene expression, decreases the insulin content and the insulin secretion [1], [5]. Under high glucose exposure, the beta islet cells show an increased cell apoptosis. Moreover, the beta cells show the lowest levels of antioxidant enzyme compared with other cells [1].
Also the endothelial cells are victims of diabetes complications [4].

2. Reactive Oxygen Species

1) What are they?

ROS is an acronym standing for Reactive Oxygen Species. This name represents different molecules and free radicals derived from oxygen.

Atomic oxygen possesses two unpaired electrons in the valance electrons. Thus, it is possible for oxygen to form radicals. The different steps of the reduction of oxygen leads to the formation of several ROS such as superoxide anion, peroxide, hydrogen peroxide, hydroxyl radical or hydroxyl ion (figure 4).

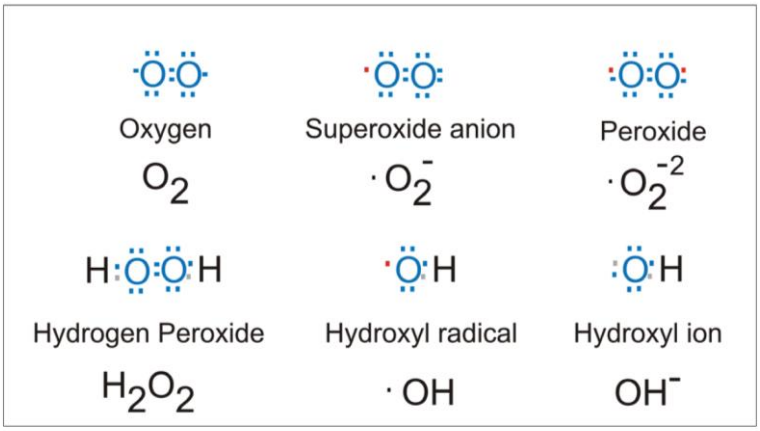

Figure 4 Oxygen and different Reactive Oxygen Species. [6]

Most of the time they are by-products of the mitochondrial electron transport respiration, oxidoreductase enzymes or metal catalyzed oxidation. These molecules are responsible for lots of harmful effects.

The mitochondria are the most productive source of ROS (95% of ROS at cellular level under physiological condition). The majority of ROS are derived from the superoxide anion $O_2^{-\cdot}$ which is produced by the mitochondrial electron transport respiration. Almost all the superoxide anions are converted to hydrogen peroxide H_2O_2 by a dismutation reaction due to an enzyme, the superoxide dismutase (SOD) (figure 5). [7]

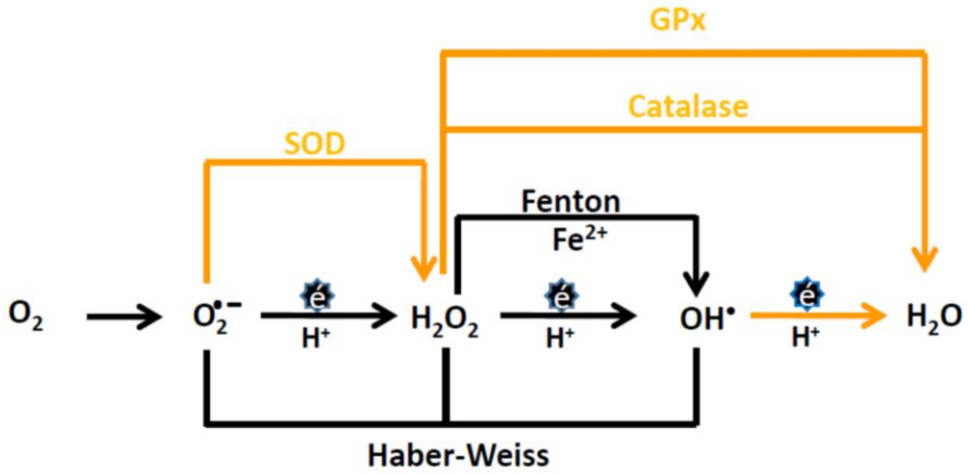

Figure 5 Origin of mitochondrial ROS. The yellow arrows represent the enzymatic detoxification SOD: superoxide dismutase, GPx: glutathione peroxidase. [7]

H_2O_2 can be neutralized by antioxidant defense (GPx, catalase) to water but a part follows the Haber-Weiss reaction and forms hydroxyl radical $OH^{\cdot}$ .The reaction is catalyzed in the presence of metallic ions and gives the Fenton reaction.

Free radicals possess an unpaired electron on the last molecular orbital which give them a high reactivity. They are represented with a dot on the figure 5.

ROS can be produced in other organelles as it can be seen in the table 1.

Table 1 Properties (t1/2, migration distance), reactivity (mode of action), formation (typical production systems), and scavenging (typical scavenging systems) of ROS in plant and animal cells. Abbreviations: APX, ascorbate peroxidase; CAT, catalase; GPX, glutathione peroxidase; PER, peroxidase; PRX, peroxiredoxin; RBOH, respiratory burst oxidase homolog; SOD, superoxide dismutase. [8]

ROS	$t_{1/2}$	Migration distance	Mode of action	Production site	Scavenging systems
Superoxide ($O^{\bullet-}_2$)	1–4 μs	30 nm	Reacts with Fe–S proteins Dismutates to H_2O_2	Apoplast (RBOHs), chloroplasts, mitochondria, peroxisomes, electron transfer chains	SOD, flavonoids, ascorbate…
Hydroxyl radical (OH•)	1 ns	1 nm	Extremely reactive with all biomolecules including DNA, RNA, lipids, and proteins	Iron and H_2O_2 (Fenton reaction)	Flavonoids, proline, sugars, ascorbate,…
Hydrogen peroxide (H_2O_2)	>1 ms	>1 μm	Reacts with proteins by attacking cysteine and methionine residues. Reacts with heme proteins. Reacts with DNA.	Peroxisomes, chloroplasts, mitochondria, cytosol, apoplast	APX, CAT, GPX, PER, PRX, ascorbate, glutathione,…
Singlet oxygen ($^1O_2$)	1–4 μs	30 nm	Oxidizes lipids, proteins (Trp, His, Tyr, Met, and Cys residues), and G residues of DNA	Membranes, chloroplasts, nuclei	Carotenoids and α-tocopherol

2) The ROS take part of an equilibrium.

ROS take part of an equilibrium between production and elimination (figure 6).

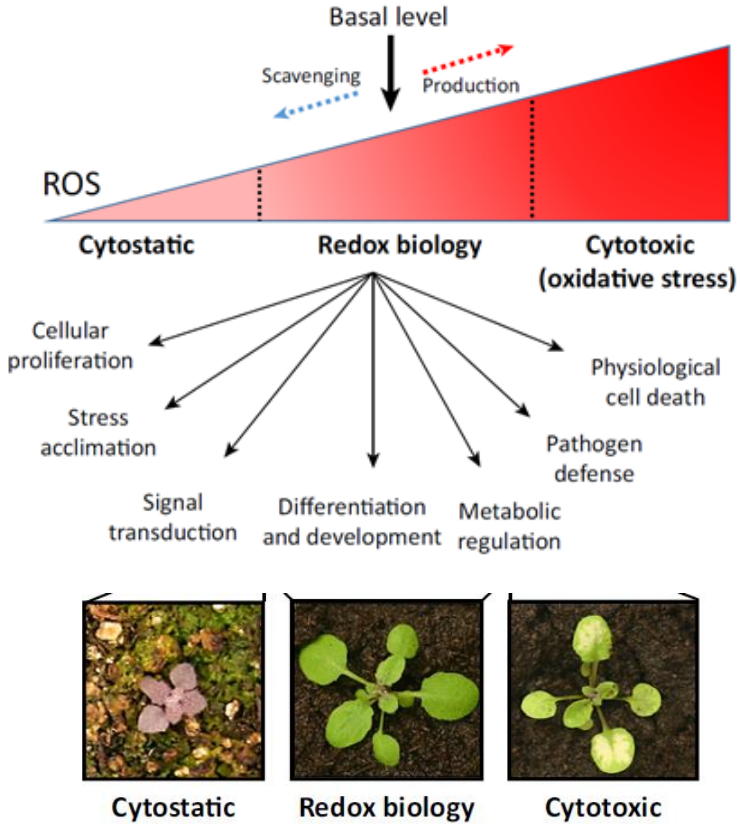

Figure 6 ROS equilibrium, between health and disease. [8]

If the redox biology is not respected, organism is threatened as it can be seen on the figure 6 (cytotoxicity).

ROS have a role in different mechanisms for example in phagocytic cells, in signal transduction or for the Redox signaling [8].

Phagocytic cells produce ROS for the bactericidal action. The production of ROS by phagocytes was originally called 'the respiratory burst' because of the rise of oxygen consumption. This process is helped by NADPH oxidase which is a complex enzyme. It is another big producer of ROS.

ROS also play a role in signaling transduction, for example nitric oxide is known to be a cell-to-cell messenger which affects blood pressure. Intra cellular ROS in conjunction with antioxidant enzymes play a role in the enzyme activity by turning it on or off with redox reactions.
ROS are required in the mitogenic signaling (relative to mitosis or the cellular division). For instance hydrogen peroxide is useful for the proliferation in response to growth factors.

When the cells proliferate, they follow a procedure, the cell cycle. There are several steps and different checkpoints. Each of them is regulated by proteins that are influenced by the oxidative state of the cell. The apoptosis of the cells is also promoted by ROS. In brief, ROS control the cell cycle via redox signaling.

But ROS can become dangerous for cells if they are present for a too long time. Organism has also its own defense mechanisms against ROS such as superoxide dismutase, glutathione and catalase [6], [39]. This provide the balance of ROS between production and elimination. An imbalanced state in favor of ROS is called the oxidative stress.

A mechanism of defense is the superoxide dismutase (SOD) which catalyzes the conversion of two superoxide anions into hydrogen peroxide and oxygen (Eq 1). After that cells convert H_2O_2 to water and oxygen which finishes the detoxification (Eq 2).

$$2\,O_2^- + 2\,H^+ \rightarrow\ H_2O_2 + \ O_2 \qquad (Eq\ 1)$$

$$2\,H_2O_2\ \rightarrow 2\,H_2O + \ O_2 \qquad (\text{Eq } 2)$$

The glutathione (GSSG), a group of enzymes, catalyzes the degradation of hydrogen peroxide to water (Eq 3) and organic peroxides to alcohols (Eq 4). It is the most important intra-cellular defense against ROS. The GSSG reduced form (GSH) is regenerated via a redox reaction by NADPH (Eq 5). A good indicator of the oxidative stress is the ratio of oxidized form of glutathione (GSSG) and the reduced form (GSH).

$$2\,GSH + \ H_2O_2\ \rightarrow GSSG + 2\,H_2O \qquad (Eq\ 3)$$

$$2\,GSH + ROOH \rightarrow GSSG + ROH + H_2O \qquad (Eq\ 4)$$

$$GSSG + NADPH + H^+ \rightarrow 2\,GSH + NADP^+ \qquad (Eq\ 5)$$

The catalase is an enzyme which degrades the hydrogen peroxide into water and oxygen (Eq 6).

$$2\,H_2O_2 \rightarrow 2\,H_2O + O_2 \qquad (Eq\ 6)$$

Vitamin C, soluble in water, is able to reduce ROS and vitamin E which is soluble in lipids has the same effects regarding ROS but it takes place in the membrane.

3. Bone disorder under diabetic mellitus

The life of bones is governed by remodeling. The bone tissue is alive and dynamic (formation, growth, mineral homeostasis…), thanks to osteoblasts and osteoclasts. They are responsible for the formation and the resorption of bone tissues respectively.

Bone mineral density is modulated by the osteoclasts, responsible for the bone resorption, and the osteoblasts which fill the cavities of osteoclasts. The osteoclasts dissolve the mineral part of the bone and enzymes dissolve the collagen part. After that, osteoblasts deposit organic matter (collagen and enzymes) where minerals (calcium, phosphate) crystalize.

The interaction between osteoblasts and osteoclasts is governed by ligand, receptor and protein.

The pre-osteoblasts (and osteoblasts) express a ligand, RANKL, and the pre-osteoclasts have a receptor, RANK. The ligand RANKL binds to pre-osteoclasts thanks to the ligand-receptor bond. This binding is a message for the pre-osteoclasts to multiplicate and fusion. This results to the formation of mature osteoclasts. Once the action of osteoclasts is done, pre-osteoblasts express a protein, the osteoprotegerin, which binds to the RANKL (preventing the bond RANK/RANKL). The pre-osteoblasts differentiate to osteoblasts and allow to fill the cavities of the osteoclasts (figure 7). After the bone remodeling, the osteoblasts can differentiate in osteocytes (bone cells) or in border cells (which cover the bone).

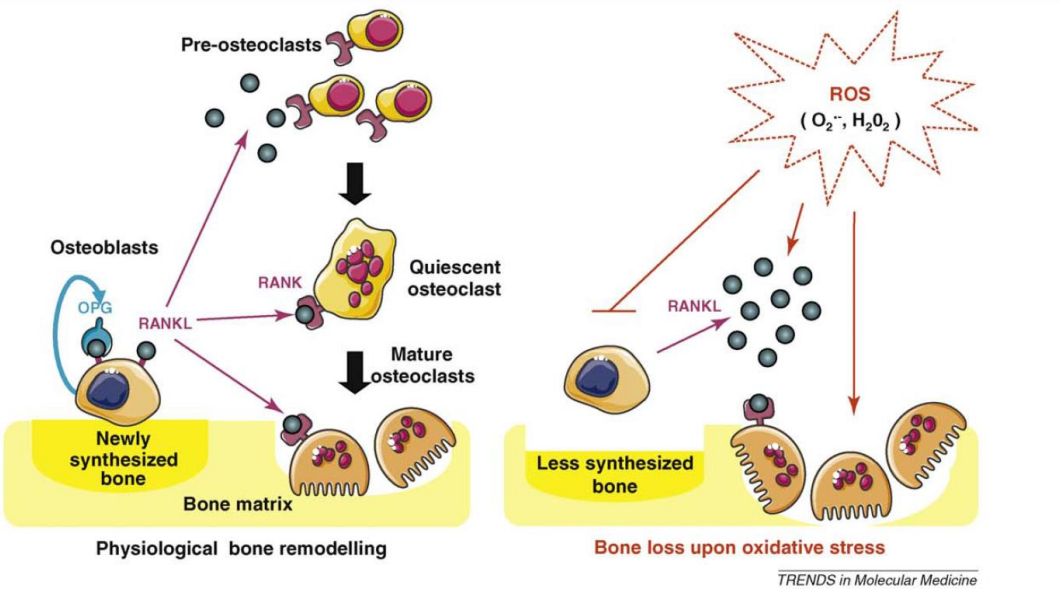

Figure 7 Bone remodeling under oxidative stress. [40]

However, under oxidative stress, the interaction between osteoblasts and osteoclasts is unbalanced and the bone formation is altered. The osteoblastogenesis is decreased whereas the osteoclastogenesis is increased. Under oxidative stress, osteoblasts produce more RANKL, increasing the osteoclasts differentiation and activities.

An equilibrium exists between formation and resorption. But with age, the activity of osteoclasts is predominant. The equilibrium is broken and it leads to a loss of bone density.

People affected by diabetes present an increased risk of fracture due to a higher level of oxidative stress. In vivo experiments show osteopenia (decrease of bone mineral density) with an increased level of oxidative stress.
Diabetes increases bone fracture and decreases bone healing and bone turnover by reducing the bone mass. One hypothesis of this, is the diabetes-induced increase in ROS. In type 2 diabetes, osteopenia is an effect of decreased mineralization. Type 2 diabetes decreases bone strength and bone mineral density, the bone fragility is highly connected to the presence of advanced glycation end-products (AGEs) in bone collagen[41]. AGEs are at the origin of the formation of oxidative stress.

In the case of implantation, a local treatment could be proposed to counterbalance the action of ROS. To enhance osteointegration an antioxidant could be used.

4. Nifedipine

1) Properties

Nifedipine is a yellow, odorless, tasteless, non-hygroscopic crystalline powder. Its formula is $C_{17}H_{18}N_2O_6$ (figure 8) and its moecular weigth is 346,3 g/mol. Its melting point is between 172 and 174 °C [9].

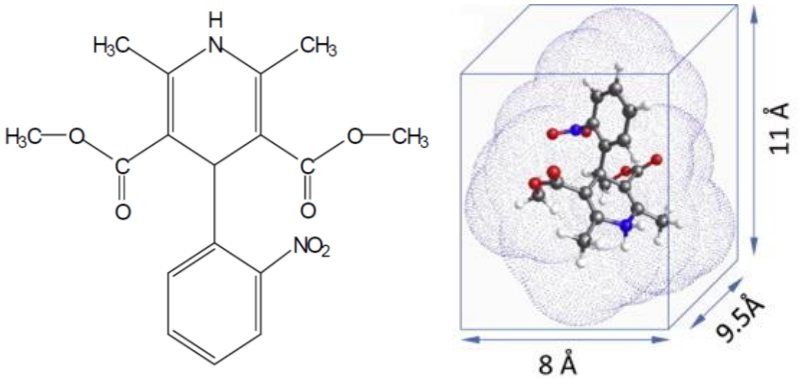

Figure 8 Nifedipine formula and dimension. [10]

The nifedipine is soluble in different solvents such as acetone, methanol or ethanol. But it is poorly soluble in water and in PBS (table 2) [9], [11].

Table 2 Nifedipine solubility

Solvent	Solubility
Acetone (20°C)	250 mg/mL
Methylene chloride (20°C	160 mg/mL
Chloroform (20°C)	140 mg/mL
Ethyl acetate (20°C)	50 mg/mL
DMSO	50 mg/mL
Methanol (20°C)	26 mg/mL
Ethanol (20°C)	17 mg/mL
Water	0,02 mg/mL
PBS (pH 7)	5,6 mg/L or 0,0056 mg/mL

Here is an infrared spectrum of nifedipine (figure 9) following by the correspondence frequencies-assignments (figure 9). The spectrum has been done using a pellet of nifedipine solidly dissolved in KBr.

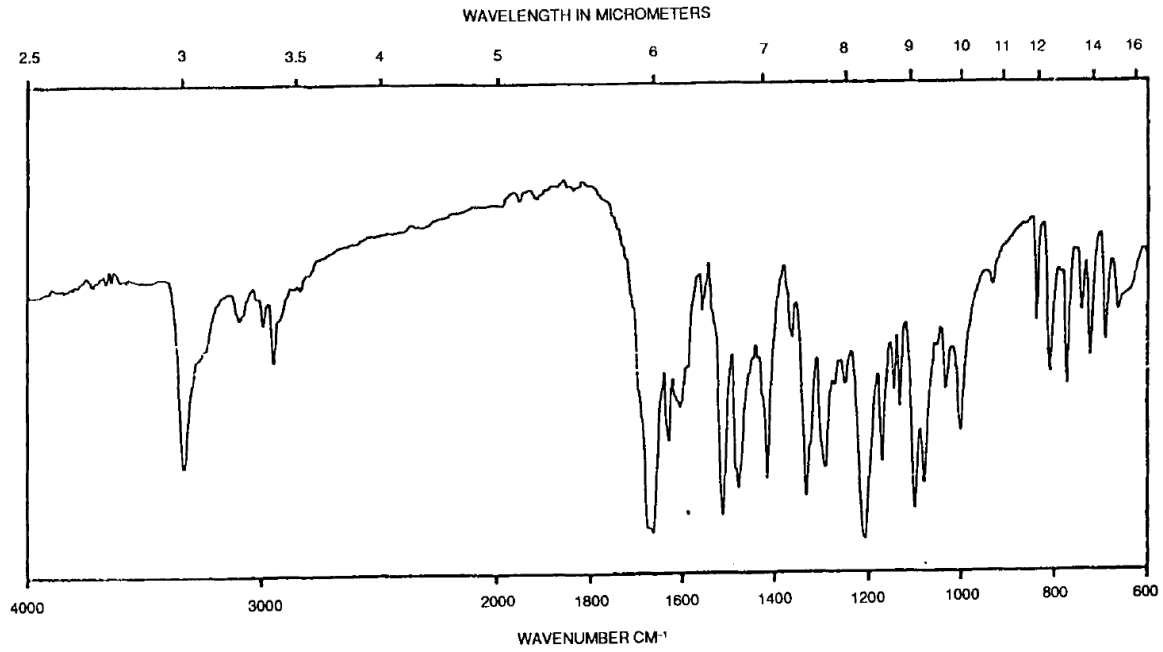

Frequency cm-1	Assignments
3331	NH stretching vibrations
3102	CH-aromatic
2931, 2842	CH-aliphatic
1689	C=O ester
1679	
1625	-C=C-aromatic
1574	
1530	NO_2
1433	
1380	$-C-CH_3$
1227	
1121	-C-O-ester

Figure 9 Nifedipine IR spectra and correlation between structural assignments and band frequencies. [12]

An example of an ultraviolet spectra of the nifedipine is given figure 10. The spectra have been processed with methanol (absorption maxima at 235 and 340 nm), HCl (maximum absorption at 238 nm) and NaOH (maximum absorption at 340).

A study has used the UV-vis spectrophotometry to analyze the nifedipine in PBS. The nifedipine shows a maximum at 238 nm using this solvent [43].

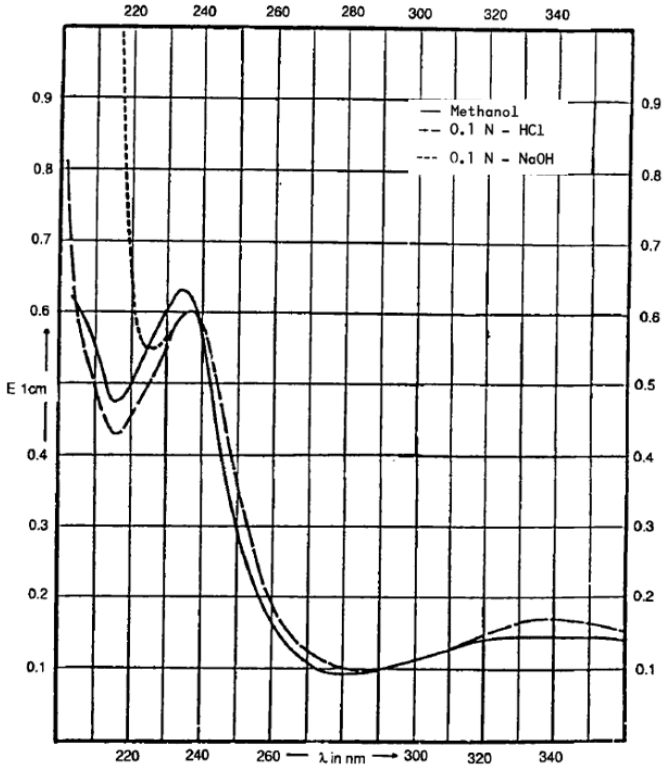

Figure 10 UV spectra of Nifedipine in different solvents. [12]

The nifedipine is a sensitive molecule. Light, elevated temperature and presence of oxidizing agent can degrade the nifedipine [13].

Under these conditions, nifedipine leads to two derived compounds: nitroso nifedipine, NO-NIF (I) and nitro nifedipine, (II) (figure 11). The photo stability of the drug depends on the irradiation wavelength, the time exposure, the intensity and the state of the formulation (solid or liquid). Nifedipine in solution is much more sensitive to light than in its solid form. Nifedipine is highly sensitive to UV-vis radiation up to 450 nm with a maximum at 380 nm with a quantum yield of about 0.5. The molecule seems to degrade following a first order reaction [13].

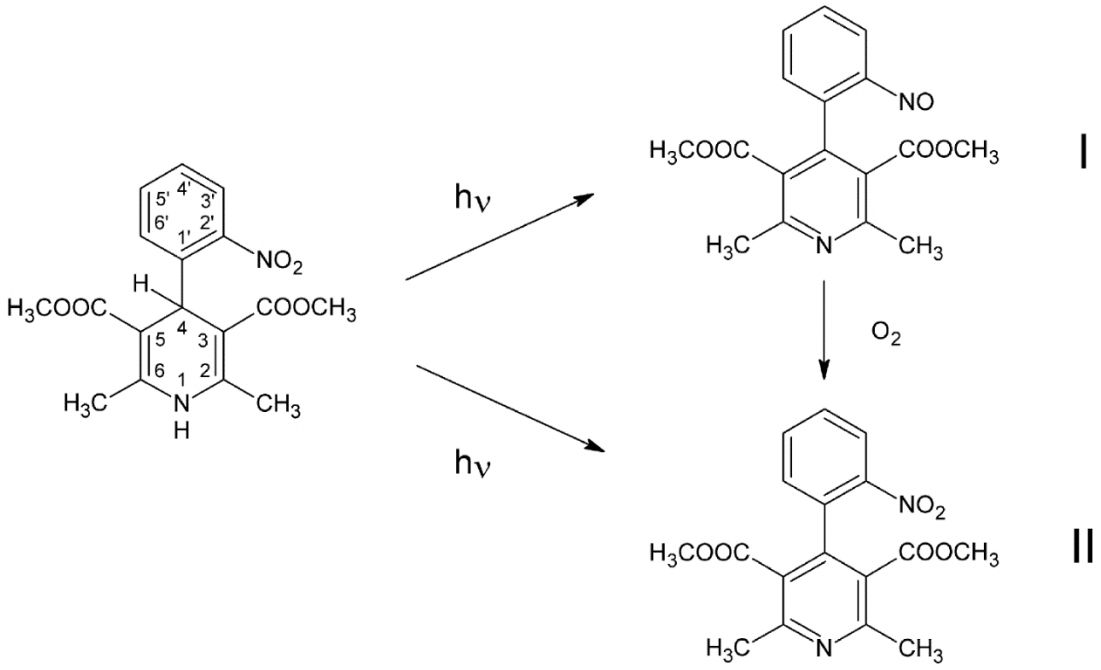

Figure 11 Derived compounds of nifedipine. [13]

The quantum yield corresponds to the number of chemical species that undergo reaction per photon of absorbed radiation of a given energy.

The stability of nifedipine under different source lights have already been studied (figure 12). A solution of nifedipine (0,01%) in alcohol was kept exposed to daylight. At the beginning, the solution was yellow and turned colorless. The nitroso compound was formed with a new absorption peak at 280 nm. [12]

Light source	k (min-1)	t50 (min)	t90 (min)
spectrotest (xenon lamp) 700-372 nm	0.198	3.5	0.5
spectrotest (xenon lamp) 700-417 nm	0.040	17	2.5
day light, november	0.015	45	7
light bulb, 40 W	0.005	135	20

Figure 12 Decomposition parameter (k, t50 and t90) of nifedipine in alcoholic solution; photodegradation with different light sources. [12]

In this table are given k, the rate constant, t50, the time required for the nifedipine to reduce to half its initial concentration and t90, the time corresponding to 10% of decomposed nifedipine.

Here, it is visible that the decomposition of nifedipine in solution under light is quite fast.

2) Medicine

➔ Calcium channel blocker

Calcium channel blockers (CCB) or calcium antagonists inhibit the entrance of calcium (Ca^{2+}) into cells. This kind of drug is mainly used to treat heart diseases or high blood pressure. Nifedipine is a derivate from dihydropyridine and is a L-type channel blocker (figure 13 a)).

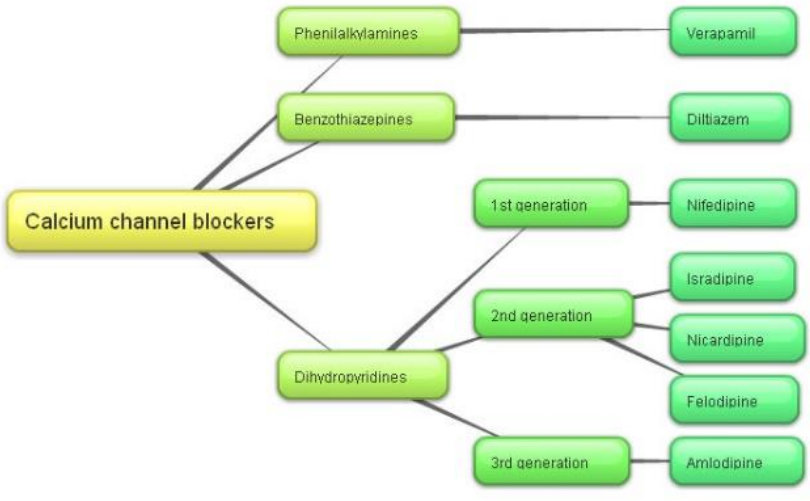

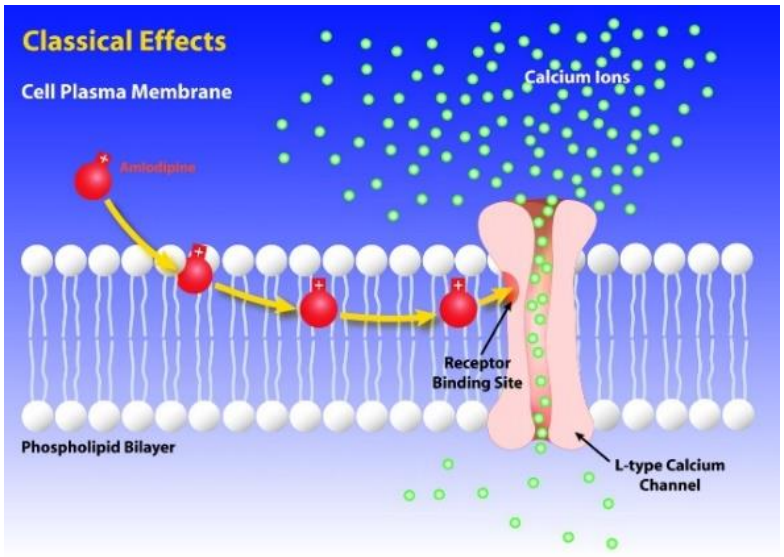

Figure 13 a) and b) : Classification of calcium channel blockers and Classical effect of L-type CCB : amlodipine [14].

Calcium ions are vital for biologic processes such as enzymatic reaction and metabolism of bones. The blocking effect of calcium antagonists is voltage-dependent, the blocking is more effective when the membrane is depolarized as voltage gate calcium channels are opened [15].
There are several kinds of calcium channel blockers: L-type for long lasting, large channel, N-type for neural, P-type for purkinje cells (neurons) and T-type for transient, tiny channel. There are at least two classifications, one which considers the percentage of inhibition and the other one the affected cells.

The mechanism of action can produce two effects, either a physical obstruction or a distortion of the membrane through a nonspecific interaction [15].

Apparently, dihydropyridine compounds bind to proteins (figure 13 b)) and cause an obstruction because of a physical connection but it seems to be more difficult than this (some dihydropyridines bind to the same site but act totally differently and open the gate) [15].

Channels, where dihydropyridines bind to, exist in different modes: 0 (channel does not open in response to a depolarization), 1 (depolarization produces low and brief opening) and 2 (depolarization produces a very high and prolonged openings). Dihydropyridines bind selectively to channel in mode 0 which favor a non-opening state [15].

➔ Antioxidant

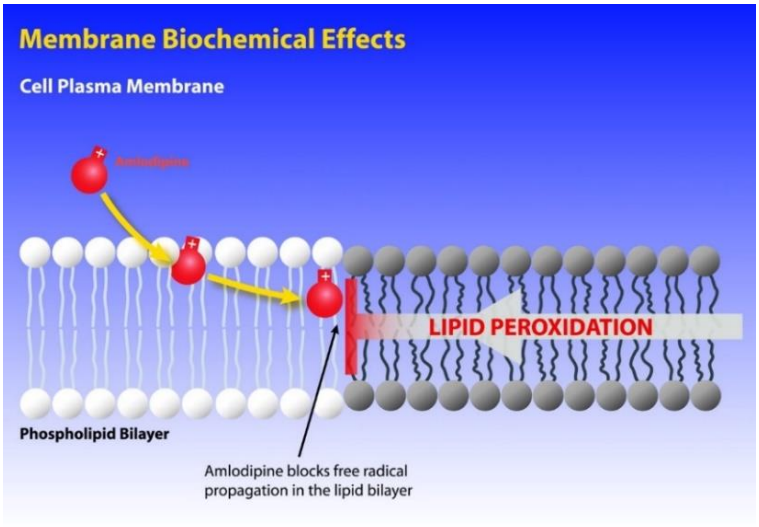

Figure 14 Schematic of the antioxidative activity of a lipophilic CCB: amlodipine [14].

Previous studies have shown the antioxidant properties of nifedipine. For example in cardiovascular diseases, the calcium blockers may provide antiperoxidative protection to cardiac membranes (cardiovascular diseases are due to the presence of free radicals in the membrane) [16]. Other studies highlighted the effects of several beta-blockers, whose nifedipine took part, on free radical

injury in endothelial cells [17]; and the effect of short or long-term treatment of endothelium with dihydropyridine calcium antagonists which results in an increase in oxide nitrite [18]. The antioxidative behavior of nifedipine is independent of the calcium channel blocking activity.

The antioxidant capacity of dihydropyridine compounds can be due to aromatic unsaturated ring moieties which provides a resonance stabilization for trapped radicals. The radicals can be neutralized by a hydrogen transfer or electron donating mechanism.
In the case of nifedipine, it contains an electron rich dihydropyridine moiety. Thus the antioxidant action may be mediated by an electron transfer process [17].

The antiperoxidative activity is correlated with the lipid solubility [14].
Lipid peroxidation can be also prevented by dihydropyridine drugs (figure 14). The prevention is related to the lipophilicity and the chemical structure of the drug. The structure facilitates proton-donating and resonance-stabilization mechanisms quench the free-radical reaction. More precisely, highly lipophilic CCBs are capable of donating protons to lipid peroxide molecules and thus blocking the peroxidation process (Eq 7). The free electron associated with the drug molecule can be stabilized in resonance structures thanks to the dihydropyridine ring.

$$LOO\bullet + DHP \rightarrow LOOH + DHP\bullet \quad \text{(Eq 7)}$$

with LOO• the lipid peroxide molecule and DHP dihydropyridine.[14]

➔ Nitroso compound

The derivative compounds of nifedipine were evaluated as toxic because they don't provide the calcium channel blocking effect.

However it has been shown that the derived compound from nifedipine has antioxidant properties. The nitroso nifedipine (compound I, figure 11), (2,6-dimethyl-4-(2-nitrosophenyl)-3,5-pyridine-dicarboxylic acid dimethyl ester) does not show hypertensive activity but antioxidant one. NO-NIF is accumulated in the membrane and converted to NO-NIF radicals. This seems to give a good protection against ROS, even better than some antioxidant (Trolox C, an antioxidant similar to vitamin E) (figure 15). Moreover, NO-NIF can be produced enzymatically without exposure to light [19].

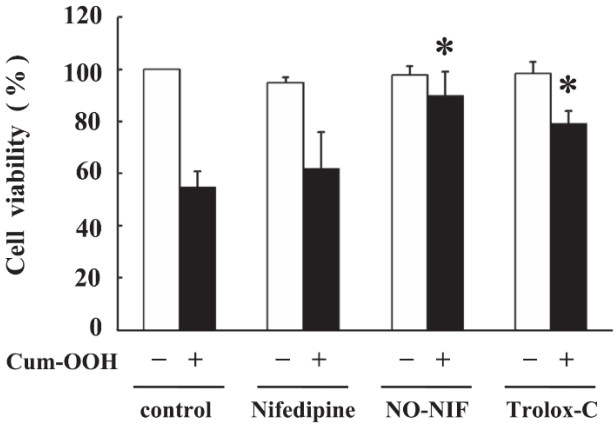

Figure 15 Protective effect on NO-NIF on Cum-OOH. [19]

This graph compares the antioxidant activity of Nifedipine, NO-NIF and Trolox-C against ROS (Cum-OOH). Nifedipine shows an antioxidant activity but NO-NIF shows a better one even better than Trolox-C.

➔ Diabetes

Nifedipine has been shown to improve cognitive functions in type 2 diabetes [20].

The drug shows an attenuation of hyperinsulinemia, which downregulates insulin receptors and reduces transport into the brain causing cognitive decline. Nifedipine could attenuate insulin

resistance and superoxide anions in the brain. Both are linked because oxidative stress increases insulin resistance.

Dihydropyridine can also be used to treat diabetic nephropathy, renal diseases which affect type 1 and type 2 diabetic people. These drugs allow a vasodilation of arterioles and has beneficial effects in term of reducing proteinuria (protein leakage in the kidney which is an evidence of an unhealthy kidney) and slowing the progression of diabetic renal failure [15].

Nevertheless, for the implant treatment, the drug could not be orally administered. The treatment will be localized near the implant. As the implant can not be simply recovered with the drug, carriers are needed. Moreover the carriers could protect the drug from degradation.

5. Nanoparticles

Nifedipine is a poorly water-soluble calcium channel blocker drug. Due to insolubility, nifedipine possesses a low bioavailability. To overcome both problems, one strategy is to use an excipient to improve the dissolution of the drug like a polymer nanosuspension, polymeric nanocapsules, or mesoporous silica as drug delivery carriers (drug adsorbs into mesopores) [1]. In this project, we will focus on mesoporous silica nanoparticles. This kind of material shows a high specific area and large pore volume. These two parameters will contribute to the efficiency of the drug loading.

The main idea is to load the nifedipine inside the particles thanks to a solvent via adsorption. And then the drug will be released.
This strategy has been already reported on bibliography [10], [21], [22], [23], [24].

1) Synthesis

The synthesis is based on a sol-gel procedure. The nanoparticle structure is obtained from a surfactant. In this study, cetyltrimethylammonium bromide (CTAB), is used (figure 16).

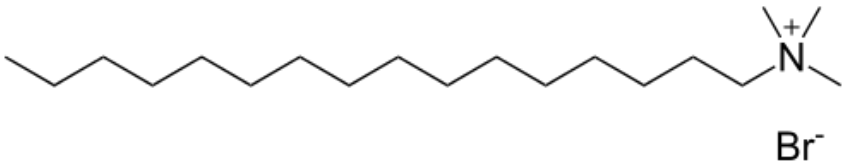

Figure 16 CTAB formula.

This kind of molecule is amphiphile, that is, with a hydrophobic part and a hydrophilic part (figure 17 a)). In water, these molecules organize themselves in micelles (figure 17 b)) to minimize the repulsive interactions between the hydrophobic part and water. Thus, hydrophobic parts gather and micelles

are formed.

They are obtained spontaneously from the critical micellar concentration (the smallest concentration needed to form micelles).

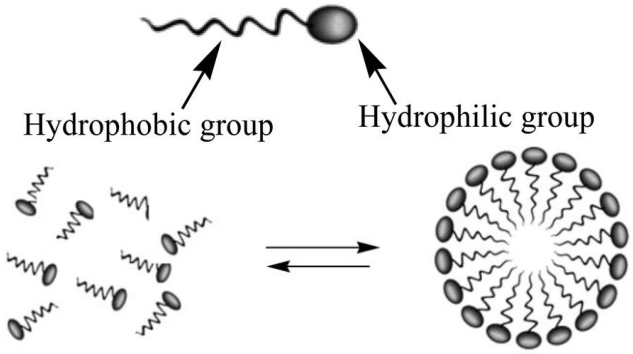

Figure 17 a) Surfactant and b) micelle morphology. [25]

The critical concentration is characteristic of each surfactant and depends on the temperature and the presence of additive in the reactive medium.

The experimental setups are very important because the form of the micelle depends on it. The structures adopted by the micelles can be spherical, cubic, lamellar or hexagonal (figure 18).

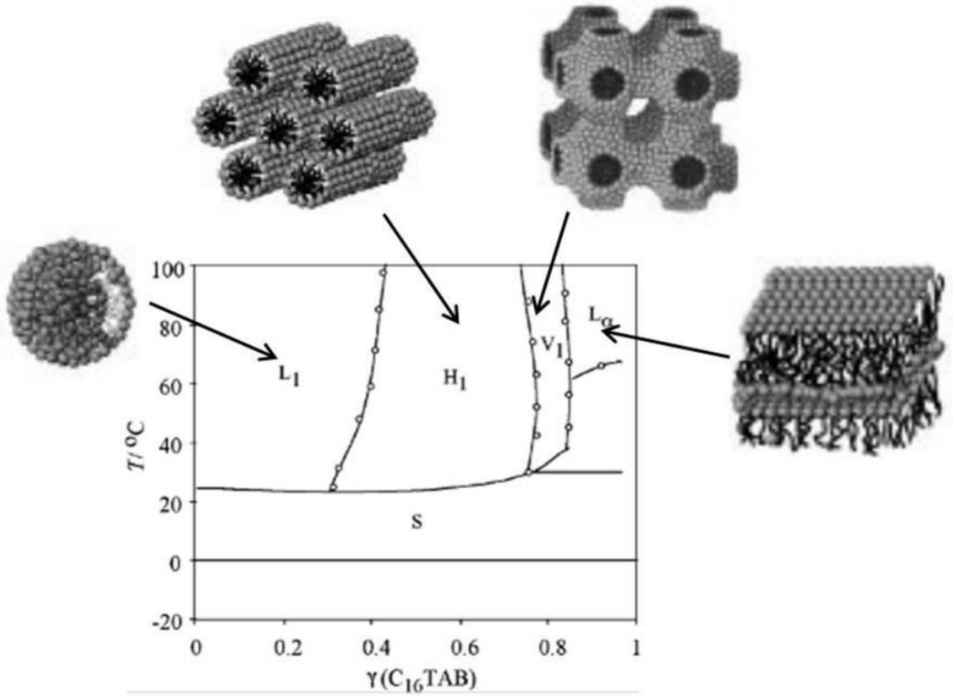

Figure 18 CTAB/water phase diagram, Temperature versus surfactant fraction. L1: isotropic liquid, H1: hexagonal phase, V1: cubic phase, Lα: lamellar phase, S: surfactant crystals. [26]

In this project, hexagonal structures are synthesized.

After the formation of the micelles, the silica skeleton is formed from the hydrolysis reaction of tetraethyl orthosilicate (TEOS, figure 19). The interaction between CTAB and TEOS is possible thanks to the head positively charged of CTA^+ and $Si\text{-}O^-$ groups.

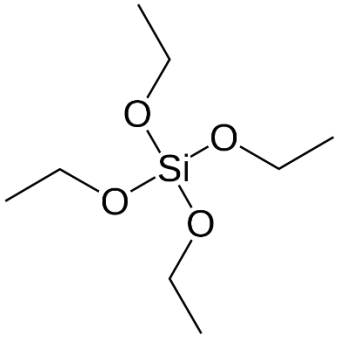

Figure 19 TEOS formula.

The formation of the nanoparticles follows three reactions: hydrolysis, alcohol condensation and water condensation (figure 20). During the first steps (hydrolysis and condensations) a solution of colloidal silica is obtained. As and when the siloxane (Si-O-Si) groups appear, a gel is formed. And finally, to obtained powder, the gel is dried and calcined.

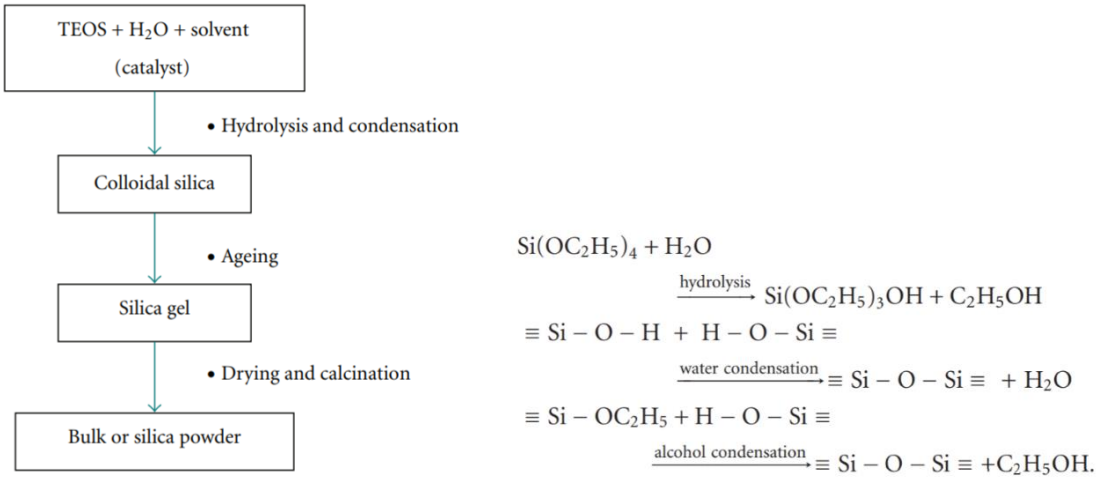

Figure 20 Different steps of the synthesis of nanoparticles. [27]

It is also possible to do hybrid mesoporous materials by functionalyzing nanoparticles. The functionalization can be done directly during the synthesis of the nanoparticles, in this case it is a co-condensation reaction. Or it can be achieved after the synthesis of the nanoparticles.

In this project, the nanoparticles have been functionalized by co-codensation. The functionalizing agent used was the (3-Aminopropyl)triethoxysilane (APTES, figure 21).

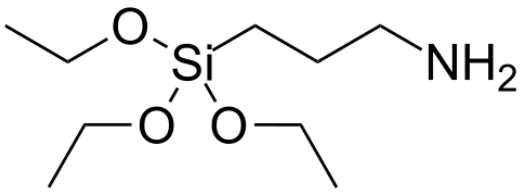

Figure 21 APTES formula.

Once the nanoparticles formed, the pores need to be cleared of CTAB. Indeed, CTAB is toxic and it fills the pores so the drug can not be loaded. The surfactant can be removed by calcination or by several washings with a solvent (such as ethanol) or by ion exchange [42]. The principle of ion exchange is to replace CTA^+ by another cation which can be further degraded. In this study, ammonium nitrate is used (Figure 22).

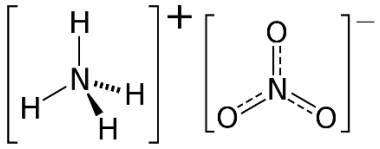

Figure 22 Ammonium nitrate formula.

The surfactant micelles and the inorganic network are linked by strong electrostatic interactions. A simple washing in solvent is not enough to remove all the surfactant. Thus NH_4^+, from ammonium nitrate, is used to replace the CTA^+ in the pores. By heating the medium, NH_3 is release in the medium and silanol groups (Si-OH) are formed (Figure 23).

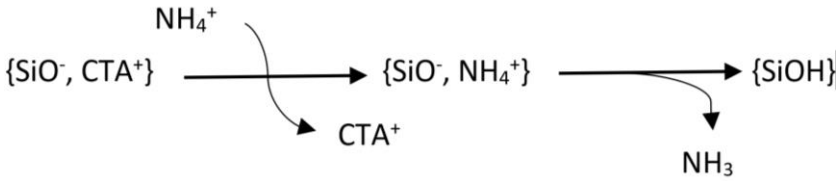

Figure 23 Extraction of CTAB with ammonium nitrate.

Finally the synthetization of the nanoparticles can be sum up by these two schemes (figure 24 a) and b)).

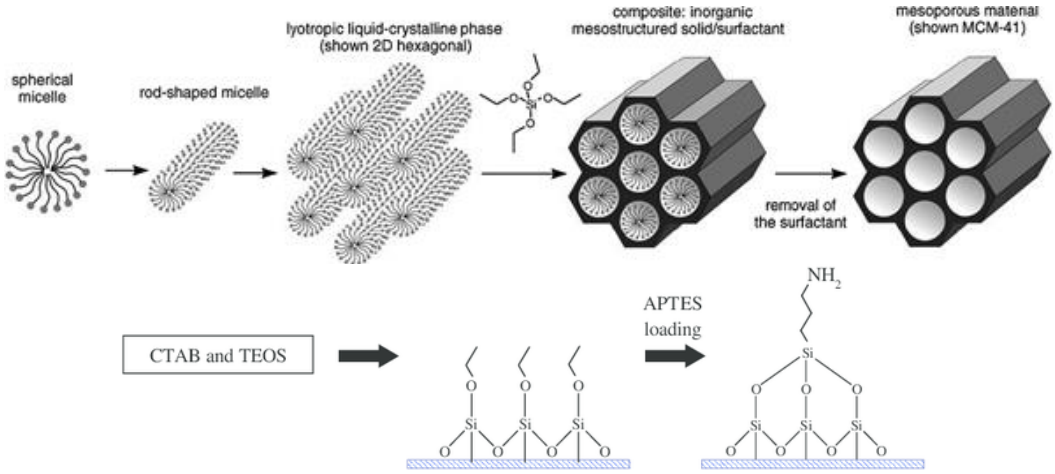

Figure 24 a) Synthesis of the nanoparticles and b) functionalization with APTES. [28], [29]

The micelles are formed and then agglomerate to form cylinders. These latter organize themselves into a honeycomb structure. The silica skeleton functionalized with APTES surrounds the micelles. And finally, the surfactant is removed, in our case using solvent and transfer reactants and not by calcination. This could affect the functionalization.

2) Drug loading and release study

The loading is performed as followed, the drug is dissolved in a solvent under stirring and nanoparticles are added. Adsorption phenomenon allows the drug to load inside the pores of the particles. [10], [21], [22], [23], [24]

The characterization of nanoparticles is performed by several techniques reported such as: UV-vis spectrophotometry, differential scanning calorimetry (DSC), thermogravimetric analysis (TG), scanning electron microscopy (SEM), transmission electron microscopy (TEM), IR Fourier transform Spectroscopy (FTIR) and X-ray powder diffraction (XRPD).

The characterization can be carried out at different steps, before the loading, during the loading or after the loading, to follow as close as possible the process.

The release is processed in vitro. Loaded nanoparticles are plunged into a buffer, as a dissolution medium, under stirring.

The characterization is performed by several techniques reported such as: UV-vis spectroscopy, DSC. A sorptometer is used to access surface area, pore volume and micropores size.

A kinetics study of the release has been done by fitting zero-order (Eq 8), first-order (Eq 9) and Hixson-Crowell formula (Eq 10) with experimental data [30].

$$Q = Q_0 + K_0 t \quad \text{(Eq 8)}$$

$$lnQ = lnQ_0 + K_1 t \quad \text{(Eq 9)}$$

$$Q^{1/3} = Q_0^{1/3} - K_c t \quad \text{(Eq 10)}$$

where Q is the amount of drug dissolved at time t, Q_0 is the initial amount of drug in solution at t=0, K_0 is the zero-order release constant, $K_1$is the first order release constant and K_c is the cube root law release constant [30].

It was demonstrated that the dissolution rate of nifedipine was increased up to 37 times compared with the bulk drug [23], [30].

2. Aims of the project

The aims of the project are the followings:

1. Synthesis of nanoparticles.

2. Study the loading of nanoparticles with the nifedipine. Compare the loading methods: evaporation and washing.

3. Characterize the loading with Fourier Transform spectroscopy (FTIR) and Thermogravimetric analysis (TGA).

4. Study the release of nifedipine. Compare different methods: dialysis, USP apparatus and tubes.

5. Characterize the release with UV-vis spectroscopy.

3. Materials and Methods

3.1. Synthesis

The synthesis of nanoparticles is composed of several steps.
The first one is the heating of 960 mL of deionized water with 2 grams of CTAB (surfactant used as a template of the nanoparticles) up to 80°C under magnetic agitation. After that 7 mL of 2M NaOH (catalyst) is added. While the mixture is under stirring and has attained 80°C, 9mL of TEOS (precursor) and 2 mL of APTES (functionalization) are mixed together and then added drop by drop in the bottle.

It is possible to have different nanoparticles by varying the amount of APTES (1, 2 or 3 mL). In a previous study, the synthetization and the characterization of these different nanoparticles have been achieved. It has been decided to continue the study with 2 mL of APTES because the corresponding nanoparticles (MSN-2-NH2) showed the best results (see previous work, TFM Florine Bodet-dubin, 2016).

The mixture is kept under magnetic agitation for 2 hours (figure 25). After that the bottle is cooled down to room temperature and finally closed and stored in a cabinet.

Figure 25 Synthesis of the nanoparticles a) before TEOS hydrolysis b) after TEOS hydrolysis.

After one week, the nanoparticles have decanted and are in the form of gel. The latter is filtered to remove all the supernatant. A Buchner filtration system is used with a membrane filter of 0.2µm. Once done, the gel is recovered in a beaker and placed in oven at 80°C for 24 hours.

After the drying time, the sample is recovered and crushed with a mortar in order to have nanoparticles in fine powder. At this step, the nanoparticles are formed but their pores are still full of surfactant. The next step is the purification of the nanoparticles.

3.2. Purification

Three different steps are followed to purify the nanoparticles.
1.5 g of nanoparticles are placed in a screw cap bottle with first 100 mL of deionized water. The mixture is placed under magnetic agitation and then filtered with a Buchner system (Figure 26). The residue is replaced in the bottle with new water and replaced under agitation.

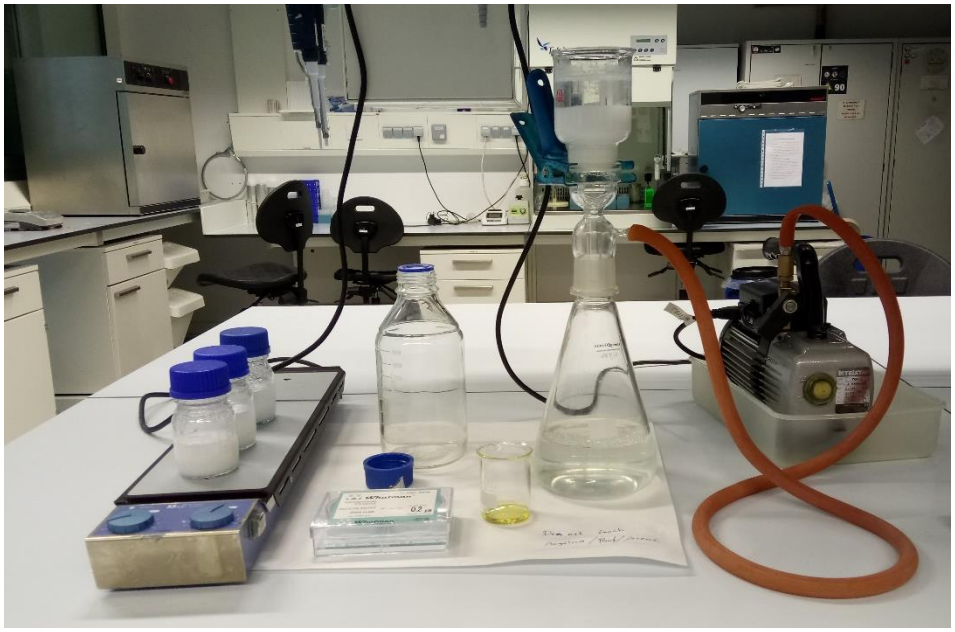

Figure 26 Buchner system and bottles of nanoparticles with deionized water under continuous stirring.

The nanoparticles are filtered three times after three washings with deionized water, three times after three washings with ethanol. And the last three ones are proceeded with 150 mL of methanol and 1.5 mg of ammonium nitrate, the all under magnetic stirring at 60°C for 24H.

After these steps, a powder of nanoparticles without surfactant is obtained.

However, to ensure that the purification has been efficient enough and no CTAB or ammonium nitrate left in the pores of the nanoparticles, a FTIR analysis has be achieved.

3.3. Loading

Method A

First of all, 60 mg of nifedipine are dissolved in 20 mL of anhydrous methanol in a 50-mL falcon tube covered with aluminum foil to prevent photodegradation of the drug. The mixture is placed under

ultra sounds for 5 min at an intensity of 10% in a cold-water bath (to prevent heat sensitivity of the drug). After that 160 mg of nanoparticles are added in the tube and placed 15 min under ultra sounds in the same cold-water bath. The tube is left under magnetic agitation for 24 hours (Figure 27). Finally, the tube is kept in the fridge sealed with parafilm.

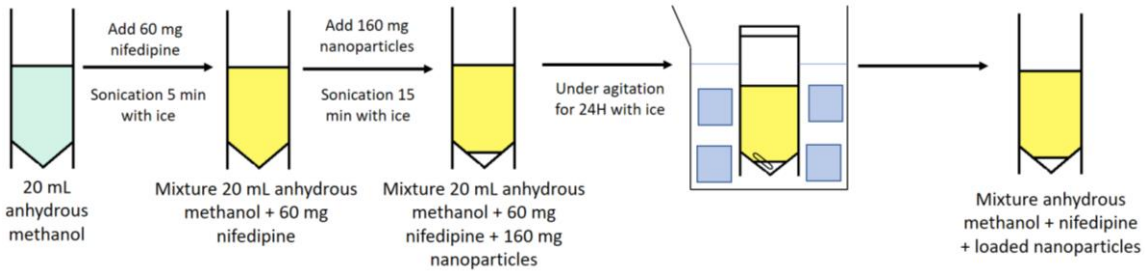

Figure 27 Schematic of the different steps of the Method A.

Method A + washing

A step of washing is added to the previous steps.

The tube from Method A is recovered and is shaken to resuspend the nanoparticles. The mixture is separated into 2 tubes (15-mL falcon tubes covered with Aluminum foil, easier to centrifuge) and the volume is adjusted to 10 mL.
Then the two tubes are centrifuged for 5 minutes at 1000 rpm. The supernatant is removed with a Pasteur pipette (as much as possible). And it is replaced by fresh anhydrous methanol (5 mL). The tubes are centrifuged for 2 min at 1000 rpm and the supernatant is directly removed with a Pasteur pipette. Deionized water is added, up to 3 mL and the tubes are centrifuged one more time with the same setups. While the tubes are in the freezer (-80°C for at least 1h30) or in liquid nitrogen, holes are done in a cap with a syringe. Once the freezing time is finished, the tubes, with the holed caps, are placed in the container of the freeze dryer (Figure 28) for the whole night (Figure 29).

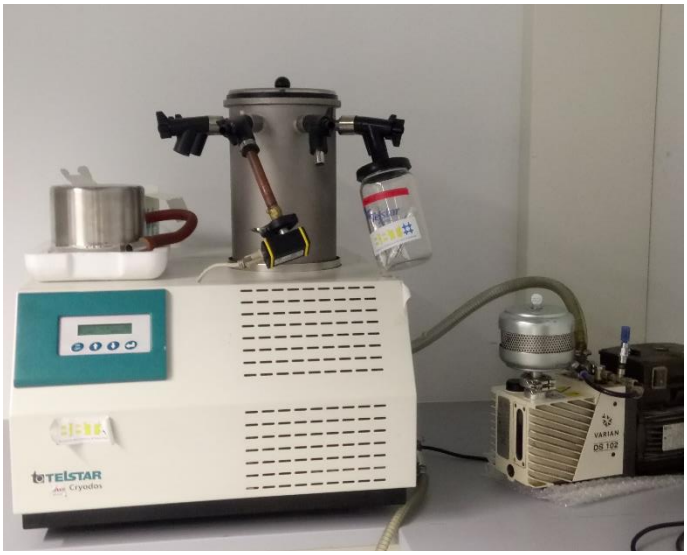

Figure 28 Photograph of the freeze dryer.

The day after, the tubes are recapped and stored in the fridge.

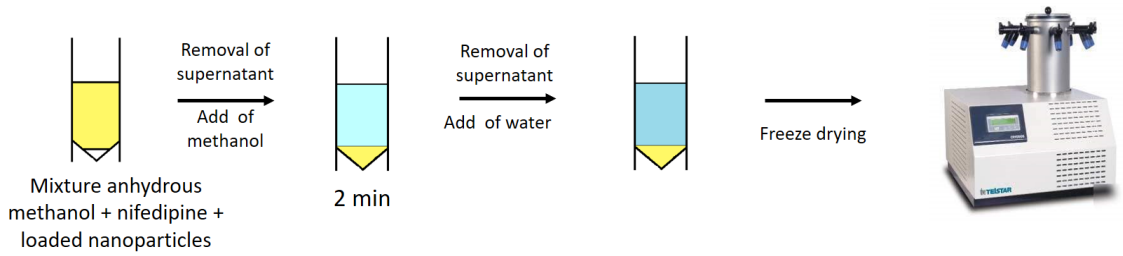

Figure 29 Schematic of the lasts steps of the Method A with washing.

Method B

60 mg of nifedipine are dissolved in 20 mL of anhydrous methanol in a 50-mL falcon tube covered with aluminum foil to prevent photodegradation of the drug. The mixture is placed under ultra sounds for 5 min at an intensity of 10% in a cold-water bath (heat sensitivity of the drug). After that 160 mg of nanoparticles are added in the tube and placed 15 min under ultra sounds in the same cold-water bath. The tube is left under magnetic agitation for 24 hours. Finally, the tube is kept in the fridge, sealed with parafilm.

The contents of the tube (anhydrous methanol with dissolved nifedipine and loaded nanoparticles) is introduced in a flask and placed in the rotary evaporator (Figure 30). The setups are 50°C for the bath temperature and 80 rpm for the rotation. The rotary evaporator is used to enhance the loading of the nanoparticles. [31]

Figure 30 Photograph of the rotary evaporator.

Once the evaporation of methanol is done, small amount (about 5 mL) of new anhydrous methanol is added to recover all the nanoparticles in the bottom of the flask and a new evaporation is proceeded with the same setups.

After that, the nanoparticles are recovered with a spatula and replaced in the same tube (Figure 31).

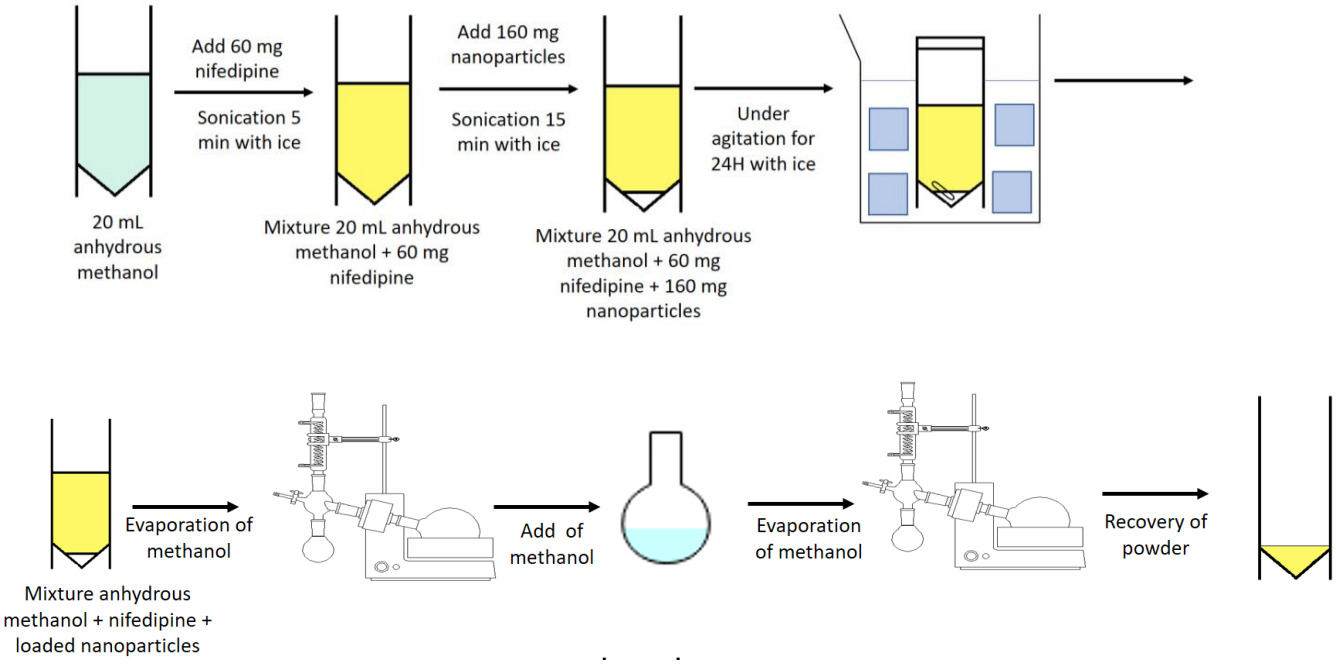

Figure 31 Schematic of the different steps of the Method B.

Method B + washing

The powder is separated into 2 tubes (15-mL falcon tubes covered with Aluminum foil) and 10 mL of deionized water is added in each. The volume is equalized with a Pasteur pipette. The two tubes are centrifuged for 5 minutes at 1000 rpm. The supernatant is very light and the nanoparticles and the nifedipine are in the bottom of the tube. The supernatant is removed with a Pasteur pipette. 5 mL of anhydrous methanol are added and the tubes are once more centrifuged for 5 minutes at 1000 rpm. The supernatant is yellow and the nanoparticles (white) are in the bottom of the tube. The supernatant is removed with a Pasteur pipette, but few milliliters are left in the tube (up to 2 mL) and deionized water is added (up to 3 mL). The tubes are centrifuged with the same setups. After that, they are placed in the freezer (-80°C) horizontally for 3 hours.
After the freezing time, the cap of each tube is replaced by parafilm with holes (done with a syringe). And the tubes are placed in the container of the freeze dyer.
The parameters of the machine are a vacuum of 0,002 mBar and a temperature of -75,1°C. The tubes are left the whole night in the freeze dryer (Figure 32).
The day after, the tubes are recovered, recapped and stored in the fridge.

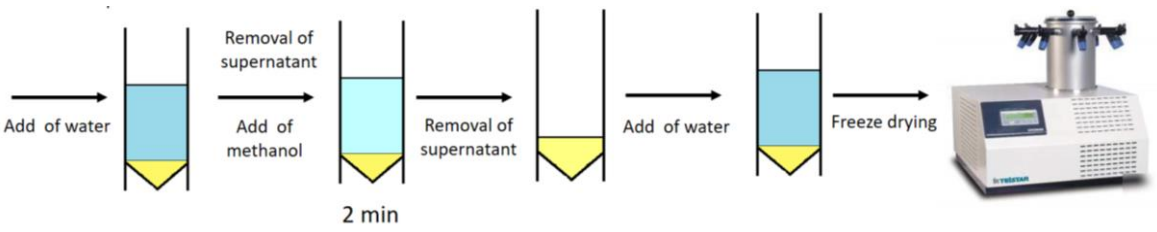

Figure 32 Schematic of the lasts steps for the Method B with washing.

Method C

60 mg of nifedipine are dissolved in 20 mL of anhydrous methanol in a 50-mL falcon tube covered with aluminum foil to prevent photodegradation of the drug. The mixture is placed under ultra sounds for 5 min at an intensity of 10% in a cold-water bath (heat sensitivity of the drug). After that 160 mg of nanoparticles are added in the tube and placed 15 min under ultra sounds in the same cold-water bath. The tube is left under magnetic agitation for 24 hours. Finally, the tube is kept in the fridge sealed with parafilm.

The contents of the tube (anhydrous methanol with dissolved nifedipine and loaded nanoparticles) is introduced in a flask and placed in the rotary evaporator. The setups are 50°C for the bath temperature and 80 rpm for the rotation. The powder is recovered with a spatula (Figure 33).

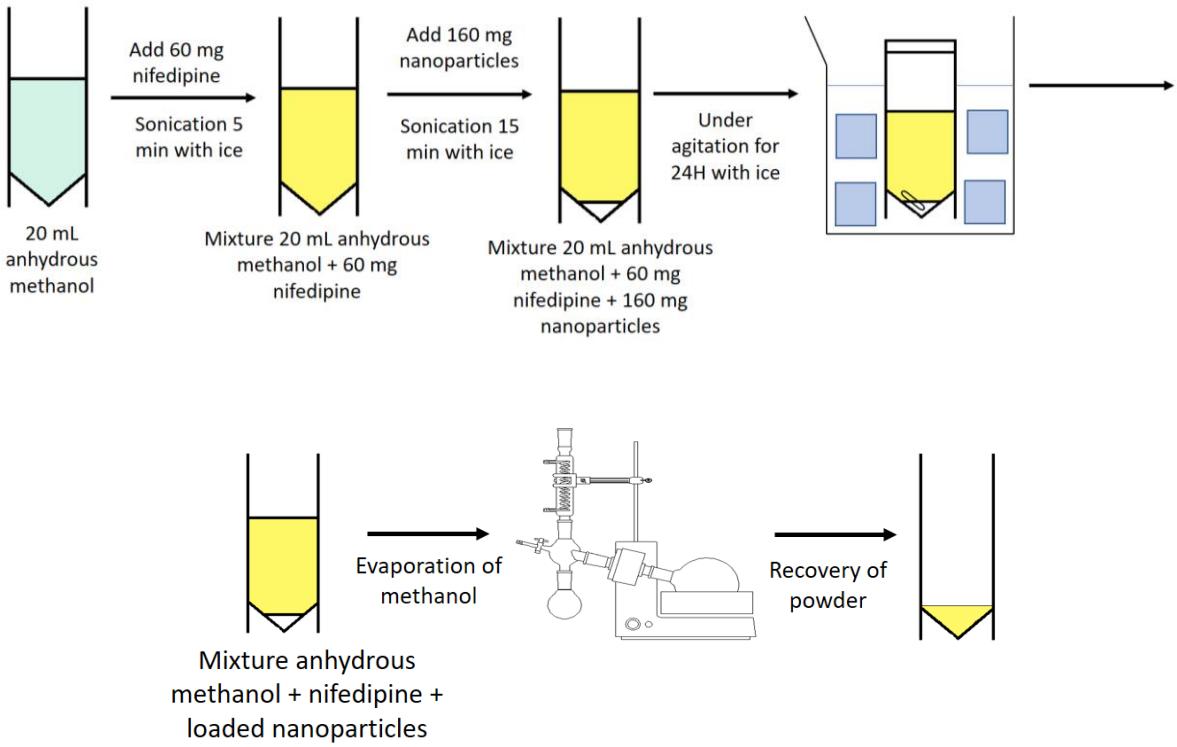

Figure 33 Schematic of the different steps for the Method C.

Method C + washing

The powder is shared in 2 falcon tubes (15 mL) with 5 mL of anhydrous methanol in each. Then the tubes are centrifuged for 2 minutes at 1000 rpm. The supernatant is directly removed with a Pasteur pipette (as much as possible). And deionized water is added, up to 3 mL. The tubes are placed in liquid nitrogen to be rapidly frozen and then introduced in the container of the freeze drier. The tubes are recovered the day after (Figure 34).

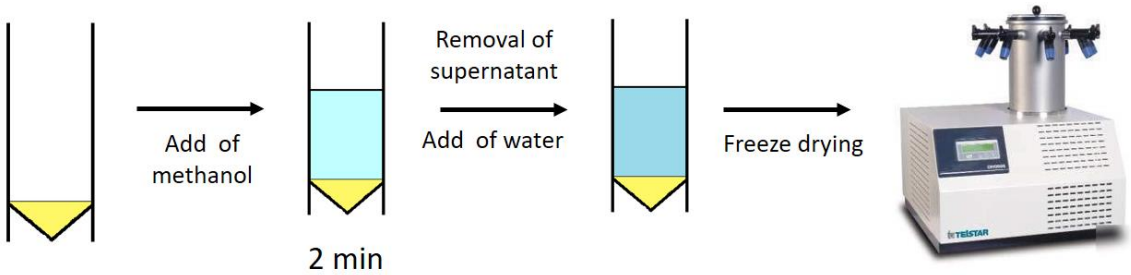

Figure 34 Schematic of the lasts steps for the Method C with washing.

From these different methods are obtained 4 samples:

MSN-2-NH2-Nif Method B
MSN-2-NH2-Nif Method B + washing
MSN-2-NH2-Nif Method A + washing
MSN-2-NH2-Nif Method C + washing

After these steps of loading and washing, a FTIR analysis has been proceeded to confirm or not the presence of nifedipine as well as a TGA to access the quantity of nifedipine present in the samples.

3.4. Release

3.4.1. Dialysis

A dialysis membrane (with a cut-off of 10 KDa) has been used to study the release of a suspension of nanoparticles (Figure 35).

Figure 35 Photograph of the dialysis membrane.

To do so, the release was studied in PBS, water with a mixture of salts which has the role to mimic the body fluids.

The membrane cassette is plunged in 200 mL of adjusted PBS (pH at 6.8) at 37°C and under agitation (Figure 36).

Figure 36 Photograph of the release experiment.

First the adjusted PSB has been prepared. A pellet of PBS was dissolved and the pH adjusted with a solution of HCl at 1 mol/L. If the pH became too low, it was possible to rectify it with a solution of NaOH at 1 mol/L.

In this study, nifedipine and loaded nanoparticles MSN-2-NH2- Nif have been used.
In the first cassette, 1 mg of nifedipine is dissolved in 3 mL of PBS which corresponds to a concentration of 0.33 mg/mL.
From a previous TGA, MSN-2-NH2-Nif (Method B) are loaded with 25.73% of nifedipine. The loading is done with 160 mg of nanoparticles.

$$100\ \% - 160\ \text{mg nanoparticles}$$
$$25.73\ \% \rightarrow 41.168\ \text{mg nifedipine}$$

In 160 mg of nanoparticles, there are 41.168 mg of nifedipine.

$$41.168\ \text{mg} - 160\ \text{mg}$$
$$1\ \text{mg} \rightarrow 3.88\ \text{mg}$$

3.8 mg of MSN-2-NH2-Nif (Method B) have been introduced into the cassette to have an equivalent of 1 mg of nifedipine.

2 aliquots were taken (2x1.5 mL) each time with a pipette. And the same volume of fresh PBS was added.

The samples have been analyzed with the UV-vis NIR spectrophotometer.

3.4.1. USP apparatus

An experiment using the USP apparatus (I and II, a recapitulative table of the different types of USP apparatus is given in Annex A) have been carried out. The equipment is commonly used to study drug delivery systems (Figure 37).

Figure 37 Photograph of the USP apparatus, the basket and the pellet.

A pellet of MSN-2-NH2-Nif (Method B + washing) have been done with a press (8 tons for 10 minutes) and placed in the basket of the USP. It was immerged in 250 mL of adjusted PBS. The jar was heated up to 37°C thanks to a water bath and under agitation thanks to the rotation of the basket (100 rpm).

Aliquots of 1 mL have been taken with the help of a syringe. An equal volume of fresh PBS was then added (another jar contains it in order to have it at 37°C directly).

To prevent evaporation, a piece of foam was placed on the cap and the syringe was always placed in the needle.

3.4.2. Tubes

In parallel an experiment with nanoparticles in powder form has been done in 50-mL Falcon tubes. This experiment models the best the final use of nanoparticles with the implant.

Figure 38 Photograph of the tubes experiment.

4 tubes have been prepared: 2 with MSN-2-NH2-Nif (Method B + washing) and 2 with MSN-2-NH2-Nif (Method A + washing).

The tubes were covered with aluminum foil to prevent photodegradation. The equivalent of 1 mg of nifedipine (to be in the range of the nifedipine solubility in PBS) for each sample has been placed in 50 mL of PBS. The tubes were placed in a water bath at 37°C under magnetic agitation (Figure 38). Before taking an aliquot, the tubes were centrifuged for 5 minutes at 1500 rcf. After that, an aliquot of 1 mL has been taken from each tube with a syringe and replace by fresh adjusted PBS.

3.5. Baseline test

A test of the baseline with PBS has been processed. The measurement was done with the spectrophotometer. The test was carried out with one cuvette (single beam measurement) filled with PBS at room temperature. Each hour the spectrum (200-400 nm) of PBS was taken for 14 hours.

3.6. Characterization

Several characterization techniques have been used during the project. The FTIR and the TGA for the loading; the UV-vis spectroscopy for the release and the baseline test.

3.6.1. FTIR

The machine used is a Fourier transform infrared spectrophotometer (Figure 39), Nicolet 6700 FT-IR. The source is a He/Ne laser.

The software used to analyze the data was OMNIC 8.
The equipment was used in transmission mode. The number of scan was 120 and the resolution 4 cm^{-1}.

The transmission mode needs a specific sample preparation. The nanoparticles (small amount) are mixed with KBr (solid dilution, one volume of nanoparticles for 4 of KBr) in a mortar. The fine powder is pressed into a pellet. The vitrification of the powder is done during the pressing which gives a translucent pellet (essential for the analysis).

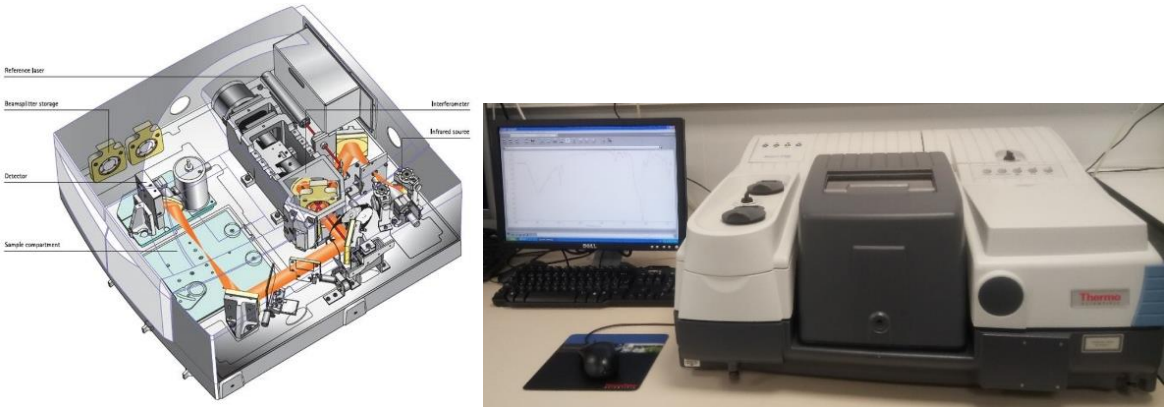

Figure 39 a) Schematic of the FTIR equipment [32], b) Photograph of the FTIR equipment.

The spectra were analyzed with the help of a table (Annex B) and previous work (see previous work, TFM Florine Bodet-dubin, 2016).

The infrared spectroscopy is based on the interaction between an electromagnetic beam and the matter. Thanks to the low energy, it enables to access the vibrational modes of atoms and molecules, and the environment of some functional groups.
The infrared spectrum of a substance can be seen as its fingerprint. Here the infrared spectroscopy is used as a qualitative analysis.

3.6.1. TGA

The machine used is a thermogravimetric analyzer TA instruments Q5 (Figure 40). The software used to analyze the data is Universal Analysis.
The sample (powder) is put in the cruiser. The latter is weighted before and after being filled, thus the mass of the sample is known.

The setups of this experiment are the following:

- ➔ Equilibrate at 30,00°C
- ➔ Isothermal for 2,00 min

➔ Ramp 10,00°C/min to 800°C

with a nitrogen flux of 60 mL/min.

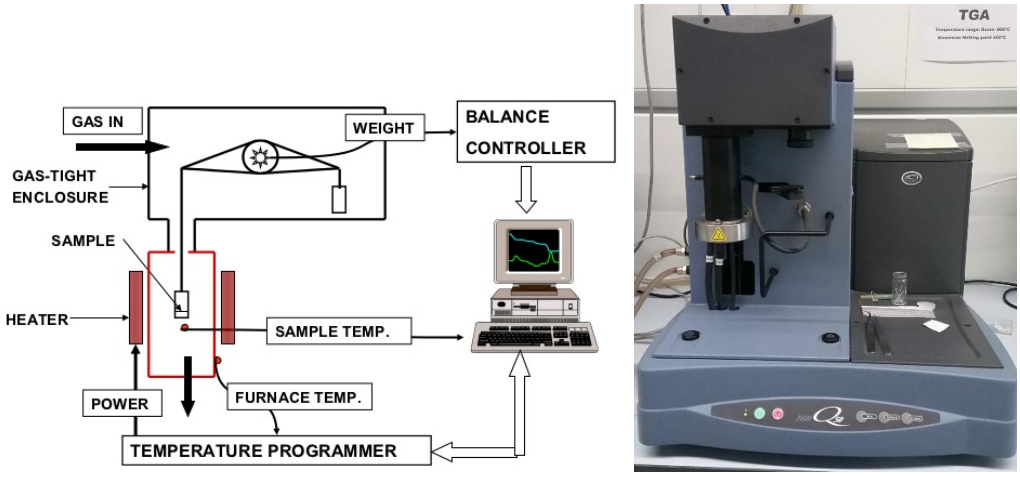

Figure 40 a) Schematic of the TGA equipment [33], b) Photograph of the TGA equipment.

The principle of the TGA is to measure the mass variation of a material as a function of time or temperature, in a controlled atmosphere. The sample, supported by the balance, is heated in a furnace under inert gas.

The TGA analysis is used as a quantitative analysis.

3.6.2. UV-vis spectroscopy

The equipment used is a UV-vis NIR spectrophotometer (Figure 41), Shimadzu UV-3600. The sources are a deuterium lamp for the UV wavelengths and a tungsten lamp for the visible and IR wavelengths. The software used to analyze the data was UV Probe Ver 2.31 Shimadzu.
The equipment is used in transmission mode. The aliquot and the reference are introduced in quartz cuvettes.

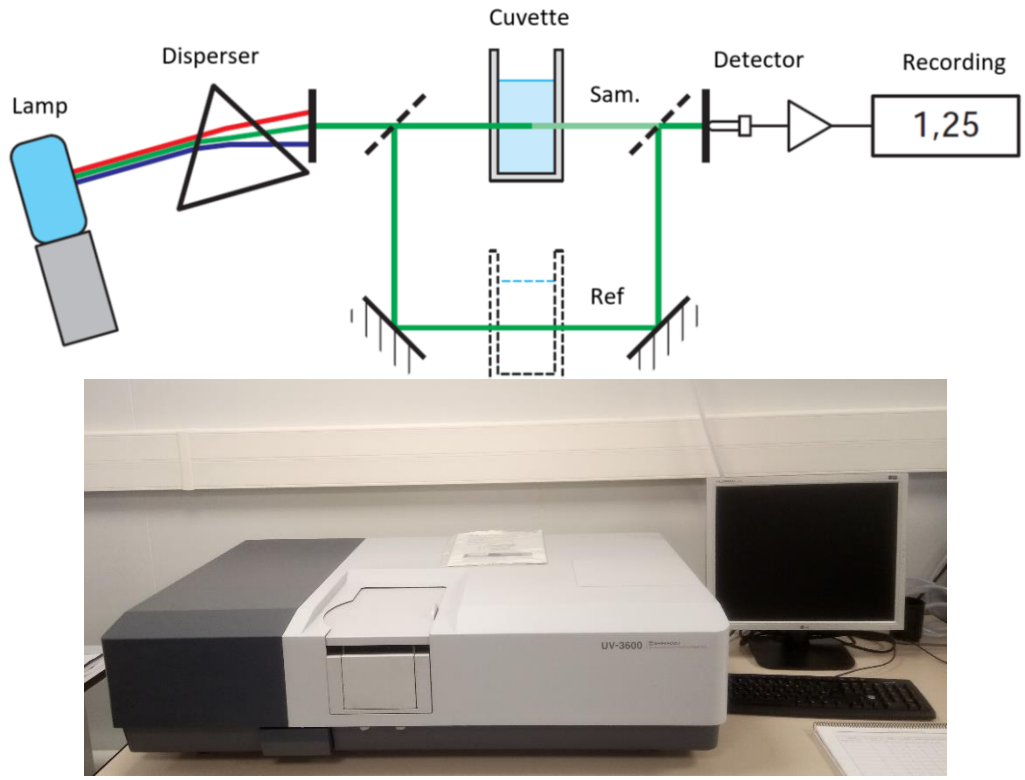

Figure 41 a) Schematic of the principle of the double beam spectrophotometer [34]*, b) Photograph of the UV-vis NIR equipment.*

The software was used in two different modes during this work: photometric (238, 288 and 338 nm) and spectrum mode (from 200 to 400 nm).

The photometric mode enables to do measurement at specific wavelengths in the spectrum. A specificity of the software is the 3-wavelength quantitation using this mode. It enables to eliminate the effects of interfering components. This formula is given as the final absorbance:

$$A = A2(\lambda1 - \lambda3) - A3(\lambda1 - \lambda2) - A1(\lambda2 - \lambda3)$$

Where A1, A2 and A3 are the absorbance of the sample at λ1, λ2 and λ3 respectively. The wavelength λ2 corresponds to the target wavelength. [35]

A typical UV-vis spectroscopy analysis follows these steps:

1. Plot the absorption spectrum of the substance to be analyzed to choose the working wavelength. It is chosen at the maximum of absorption to reduce the position of the repeatability error (Figure 42).

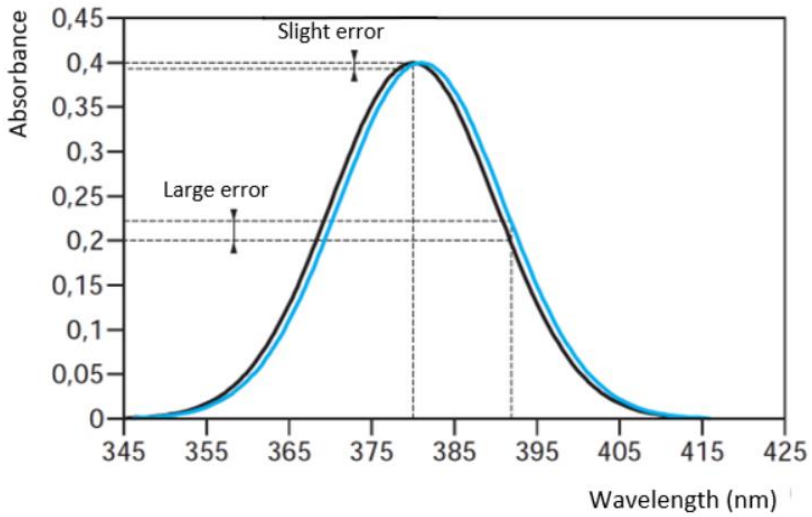

Figure 42 Graph which emphasizes the repeatability error.[34]

2. Adjust the wavelength at the working wavelength.
3. Do a calibration curve with standards (at least 5 with the blank). The blank is the solution used without the substance to dose. The calibration curve allows to access the molar attenuation coefficient, ε_λ, at one wavelength thanks to the slope of the curve (linear, if the blank is included).
4. Measure the samples absorbance regarding the blank.
5. The concentration is determined with the Beer Lambert law (Eq 11):

$$C = \frac{A}{\varepsilon_\lambda l} \qquad (Eq\ 11)$$

The UV-vis spectroscopy is based on the interaction between an electromagnetic beam and the matter. The energy can reach the energy level required for the excitation of atoms, this method enables to access electronic modes of the molecules. The UV-vis spectroscopy is used as a quantitative analysis.

4. Results and discussion

4.1. Purification

4.1.1. FTIR

An infrared analysis has been processed to ensure that the nanoparticles were enough washed and there was no more CTAB nor ammonium nitrate (Figure 43). The step of purification is to remove CTAB with the help of ammonium nitrate. But for the future it is important that both CTAB and ammonium nitrate have been eliminated during this process.

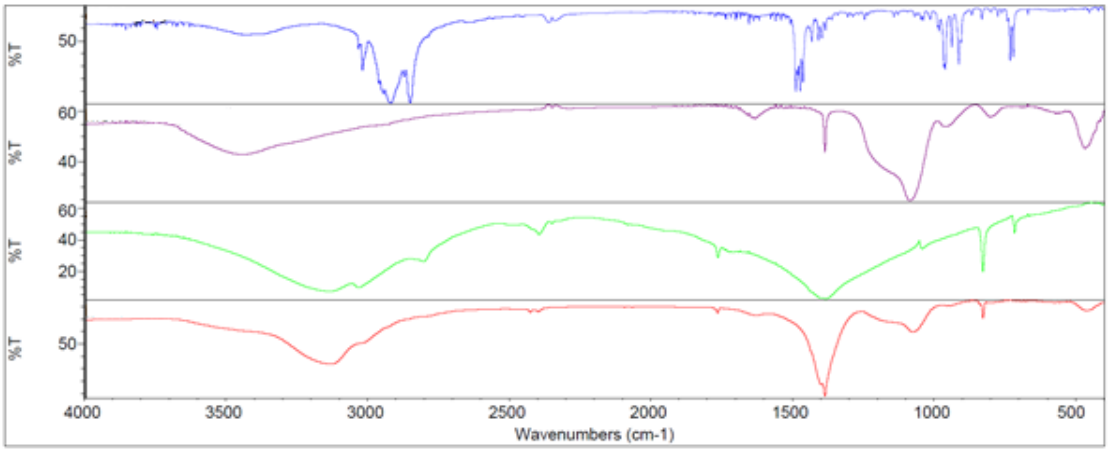

Figure 43 FTIR spectra of CTAB (blue curve), clean nanoparticles (purple curve), ammonium nitrate (green curve) and dirty nanoparticles (red curve)

The purple curve corresponds to clean nanoparticles. The band at 3439 cm^{-1} and the peak at 961 cm^{-1} correspond to silanol (Si-OH), the peak at 1630 cm^{-1} correspond to amine (R-N-H_2), the peak at 1384 cm^{-1} corresponds to alkane (C-C), the band at 1083 cm^{-1} and the peaks at 799 and 464 cm^{-1} correspond to Si-O-Si.

Whereas the red curve shows us dirty nanoparticles. We can see that the red curve is affected by the green one (ammonium nitrate) but not by the blue one (CTAB).
If we compare the purple curve with the red one we can see that the band at 3439 cm^{-1} is shifted to 3128 cm^{-1}. At 1384 cm^{-1}, a peak appears and the band of Si-O-Si is dramatically reduced as well as the peak at 457 cm^{-1}. These changes are due to the presence of ammonium nitrate. In the red curve, we recognize three different peaks of ammonium nitrate, the band at 3136 cm^{-1} (which causes the shift), the peak at 1381 cm^{-1} (which is predominant on the band of Si-O-Si at 1091 cm^{-1} and 457 cm^{-1}) and the last one at 825 cm^{-1}.

However we do not see any influence of the bleu curve on the red one. In this case, the nanoparticles were polluted by ammonium nitrate but not by the CTAB.

Regarding these results, nanoparticles have been washed one more time only in anhydrous methanol at 60°C for 24 hours. A new FTIR analysis has been processed after this washing to ensure the cleanliness of the nanoparticles.

4.2. Loading

4.2.1. FTIR

Another infrared analysis has been carried out to check the presence of nifedipine after the loading of nanoparticles (Figure 44).

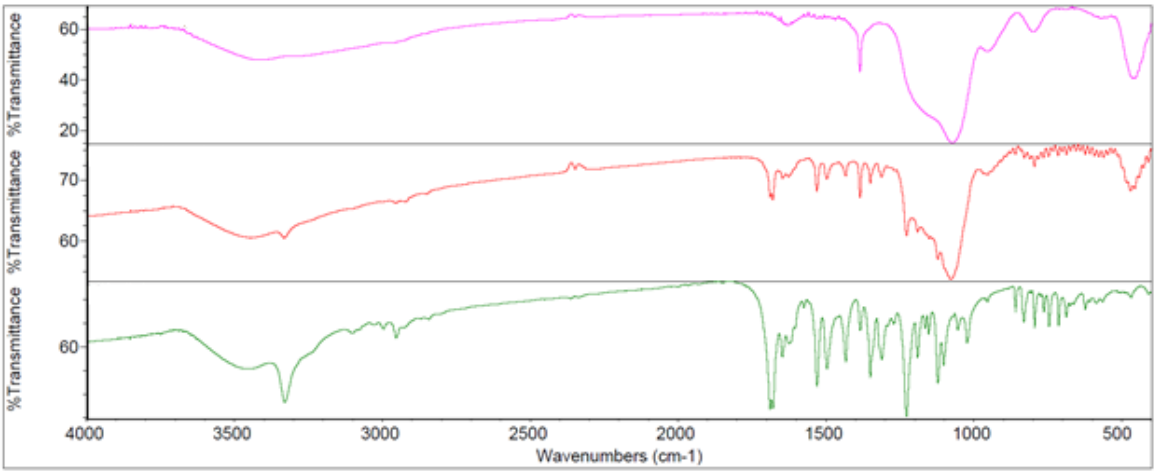

Figure 44 FTIR spectra of unloaded nanoparticles (pink curve), loaded nanoparticles (red curve) and nifedipine (green curve).

The green curve corresponds to nifedipine, the pink curve is the spectrum of unloaded nanoparticles and the red one of loaded nanoparticles.

On the red curve, we can recognize peaks of nifedipine for example at 3332 cm^{-1}, at 2953 cm^{-1} and at 1679 cm^{-1}. In the region below 1700 cm^{-1}, a multitude of peaks of the nifedipine are reported on the spectrum of loaded nanoparticles.

The curve of unloaded nanoparticles is modulated by the curve of nifedipine and gives the curve of loaded nanoparticles.

A last infrared analysis has been done to emphasize the difference between two methods (Method B+ washing and Method A + washing, Figure 45).

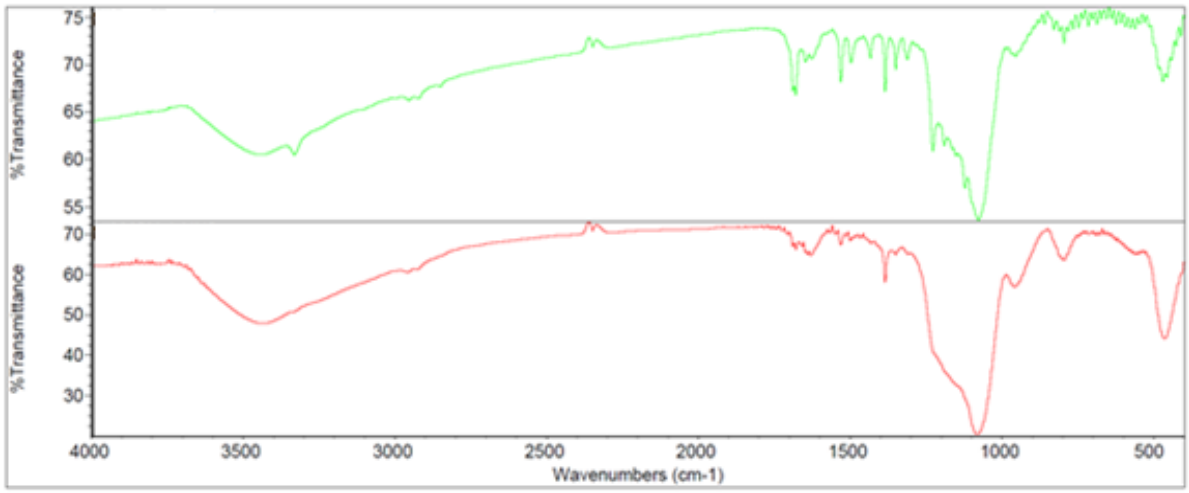

Figure 45 FTIR spectra of MSN-2-NH2-Nif (Method B + washing) (green curve) and MSN-2-NH2-Nif (Method A+ washing) (red curve).

The two curves are obtained with two different methods, in the case of the green curve (Method B + washing), the loading has been achieved with 2 sessions of rotary evaporator and washing whereas in the case of the red curve (Method A + washing), no session of evaporation and one washing have been done.

The green curve can be compared with the previous red curve of loaded nanoparticles. The same peaks, due to the presence of nifedipine, are found in both curves. However, here, the red curve (MSN-2-NH2-Nif Method A + washing), shows that much smaller nifedipine peaks. It shows that in the case of the Method A + washing there is less nifedipine than in the Method B + washing. This can be explained by the presence or not of the rotary evaporation sessions which enhance the loading.

4.2.2 TGA

A thermogravimetric analysis has been processed to have a quantitative measurement of the nifedipine present with the nanoparticles (Figure 46).

With this analysis, it is possible to access the percentage of loading thanks to the following formula [36].

$$Nifedipine\ loading = \frac{\%\ mass\ loss\ loaded\ samples - \%\ mass\ loss\ empty\ samples}{\%\ mass\ loss\ pure\ drug} * 100$$

The four samples have been tested.

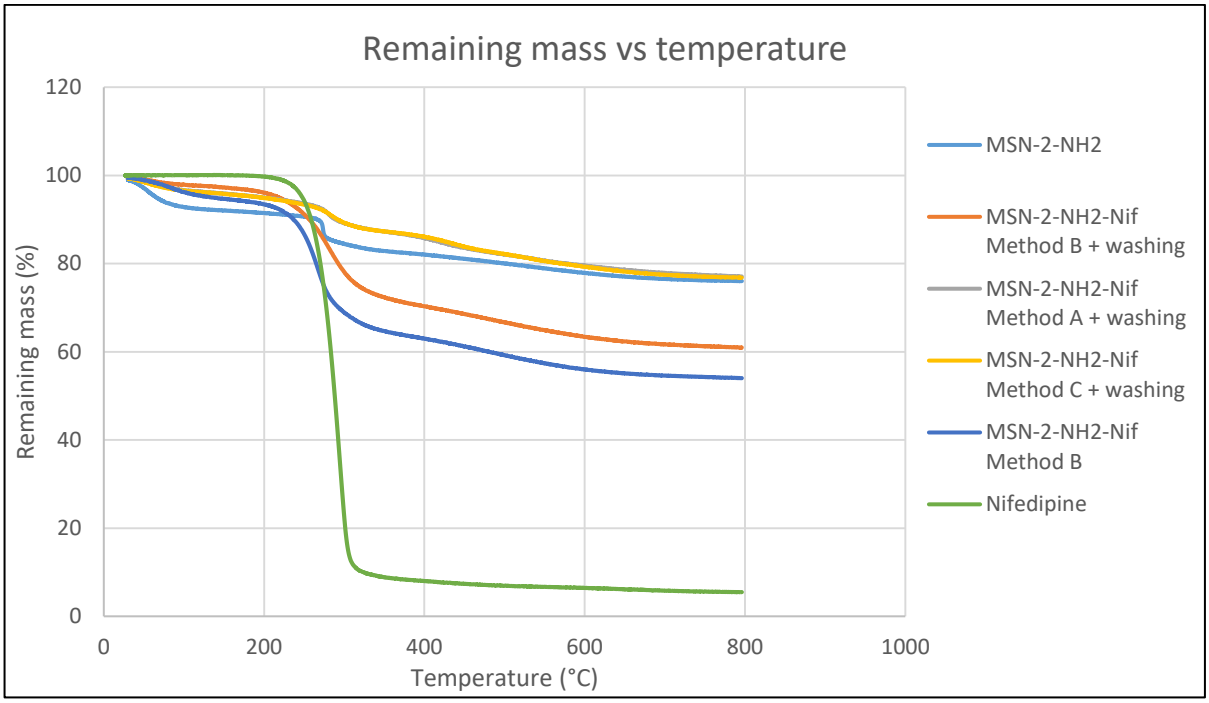

Figure 46 TGA curves of MSN-2-NH2, MSN-2-NH2-Nif (Method B, Method B + washing, Method A + washing and Method C + washing)

The mass loss of MSN-2-NH2 is due to the functionalization with APTES.

The four curves, blue, orange, grey (under the yellow curve) and yellow are the nanoparticles loaded with the different methods, respectively, the Method B, Method B + washing, Method A + washing and Method C + washing. Here, the influence of the method on the final amount of nifedipine is clearly visible.

The blue curve shows the higher quantity of nifedipine. It can be explained because the loaded nanoparticles have just been treated with the rotary evaporator. Only the methanol was evaporated and all the nifedipine not loaded inside the nanoparticles stayed there. So in this measurement, the mass loss corresponds to the nifedipine which is inside and outside of the pores.

The orange curve shows a less important mass loss than the blue one. It can be explained by the removal of the supernatant. A part of the nifedipine unloaded has been removed.

The grey and yellow curves are above the MSN-2-NH2 curve. Here, it seems that there is no nifedipine in the samples. The difference with the two previous curves is the removal of the supernatant.
In the Method A + washing (grey curve), the supernatant was removed and the nanoparticles directly freeze dried. Whereas in the Method C+ washing (grey curve), the methanol of the supernatant was

evaporated with the rotary evaporator, the nanoparticles recovered and plunged in fresh methanol. The supernatant was removed and the nanoparticles freeze dried.

With two different methods, two similar curves are obtained.

The percentage of loading has been calculated for each sample (Table 3), the detailed calculations are given in annexes (Annex C).

Table 3 Loading percentage of each sample.

	Method B	Method B + washing	Method A + washing	Method C + washing
% loading	26.86	21.28	2.97	3.12

It can be seen with the Method A + washing and C + washing that a very small amount of nifedipine is present. The fact that the grey and yellow curves are above the unloaded nanoparticles can be due to humidity (present in unloaded particles and less in loaded nanoparticles).

The loading has been done with 60 mg of nifedipine with 160 mg of nanoparticles. The nifedipine represents 37.5% of the weight of the nanoparticles. In the method B, all the nifedipine is recovered with the nanoparticles. However, with the TGA, we can see that only 26.86% is present. A difference of 10,64 mg left. It may be because of the recovery of the powder from the flask (loss of sample). Or it can be because of the homogenization of the powder. If it is not well homogenized, more nanoparticles can be taken for the measurement and modify a bit the percentage.

4.3. Release

4.3.1. UV-vis Spectroscopy

Calibration curve

The calibration curve (Figure 47) has been obtained from a solution of nifedipine in PBS at 4 µg/mL at room temperature and dissolutions. The curve has been fitted with a linear one. The solubility of nifedipine in PBS is 5.6 µg/mL.

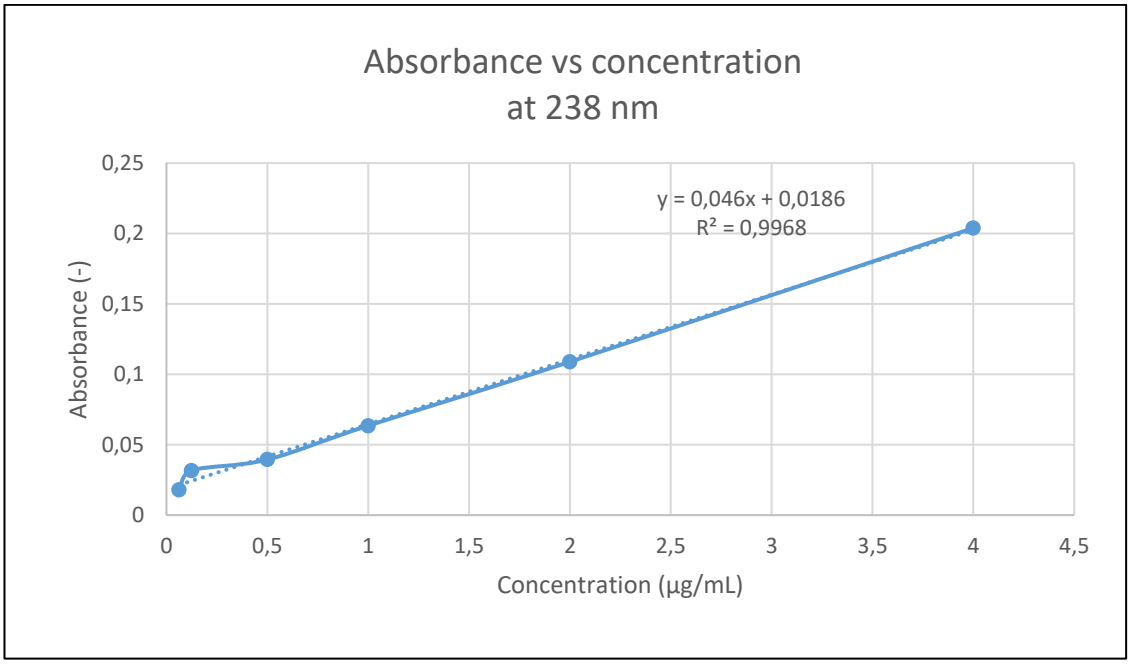

Figure 47 Graph of the calibration curve.

The calibration curve gives the absorbance as a function of the concentration at 238 nm.

Dialysis release

Here are the results of the dialysis experiment (Figures 48 and 49).

The first experiment was done with nifedipine as a control experiment.

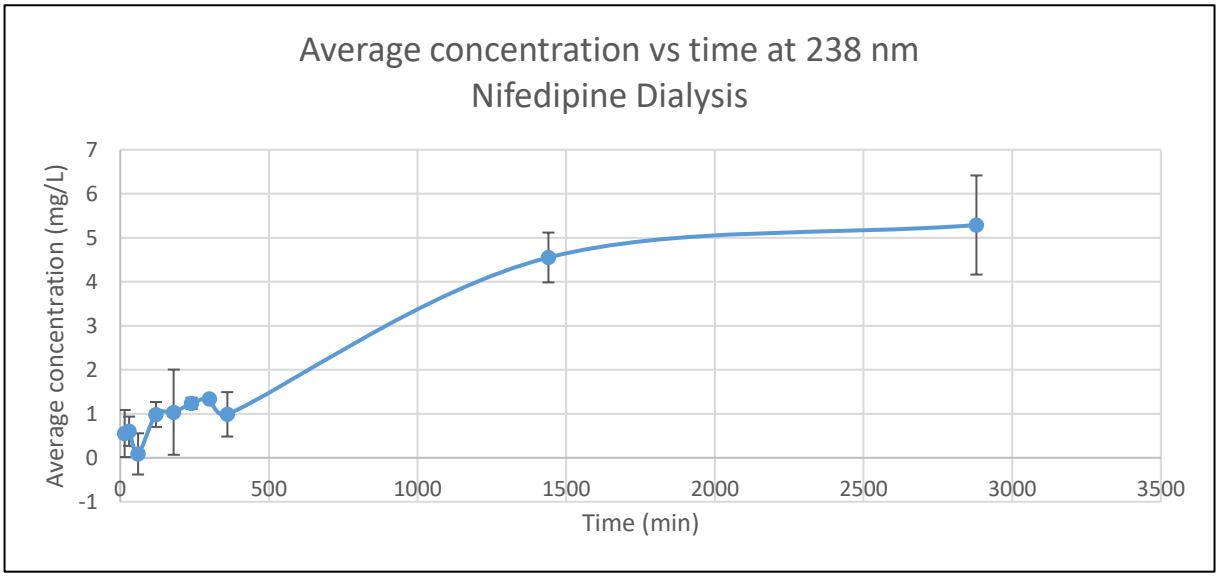

Figure 48 Evolution of the concentration with time for the Dialysis release study.

The concentration of nifedipine increases with time. It can be said that there is a release. The biggest quantity of released nifedipine is between 360 and 1440 minutes. After 1440 minutes, it increases a bit. It is possible that the release of nifedipine was not finished. The drug had two barriers to pass through to be released: the nanoparticles and the membrane. So the release can be slow.

The highest concentration reached by nifedipine is 5.29 mg/L. But the initial concentration in the membrane was 333 mg/L which is much higher than the concentration in the release medium. It is possible that the membrane was not adapted to the drug and retained it.

Here are the results for the study of nanoparticles in the membrane. This was done with the Method B. The nanoparticles were used in powder-form.

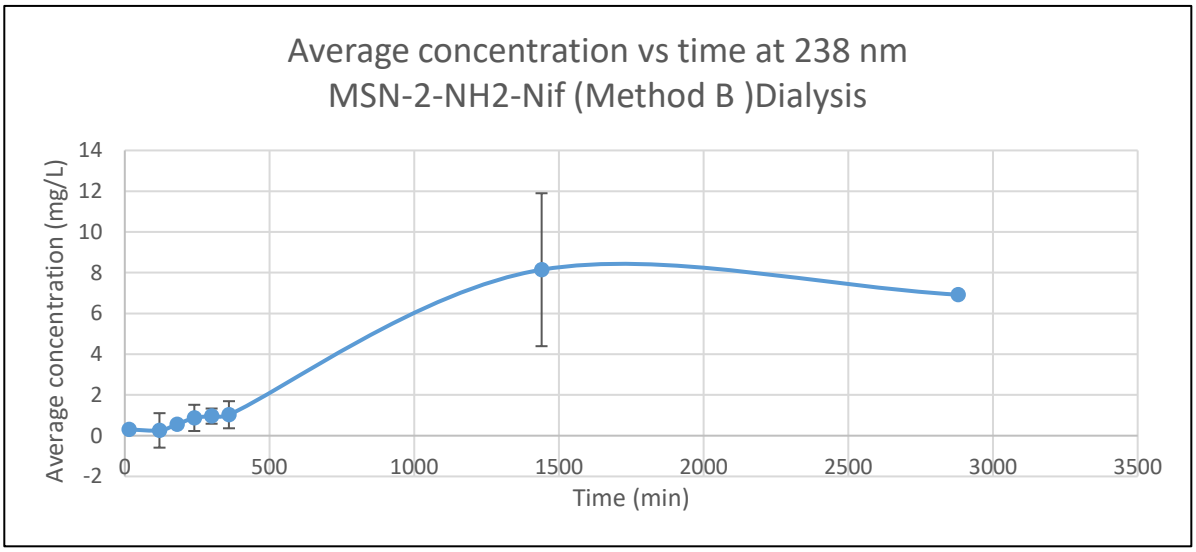

Figure 49 Evolution of the concentration with time for the Dialysis release study.

The concentration slowly increases from the first point to 360 minutes. And then a high increase of the concentration is seen from 360 to 1440 minutes. After this time, the concentration of nifedipine decreases. As the concentration of the nifedipine increases, it can be said that there is a release.

The highest concentration reach by the nifedipine is 8.15 mg/L.

USP release

Here are the results for the study of nanoparticles in the USP apparatus (Figure 50). This was done with the Method B + washing. The nanoparticles were used in a pellet form.

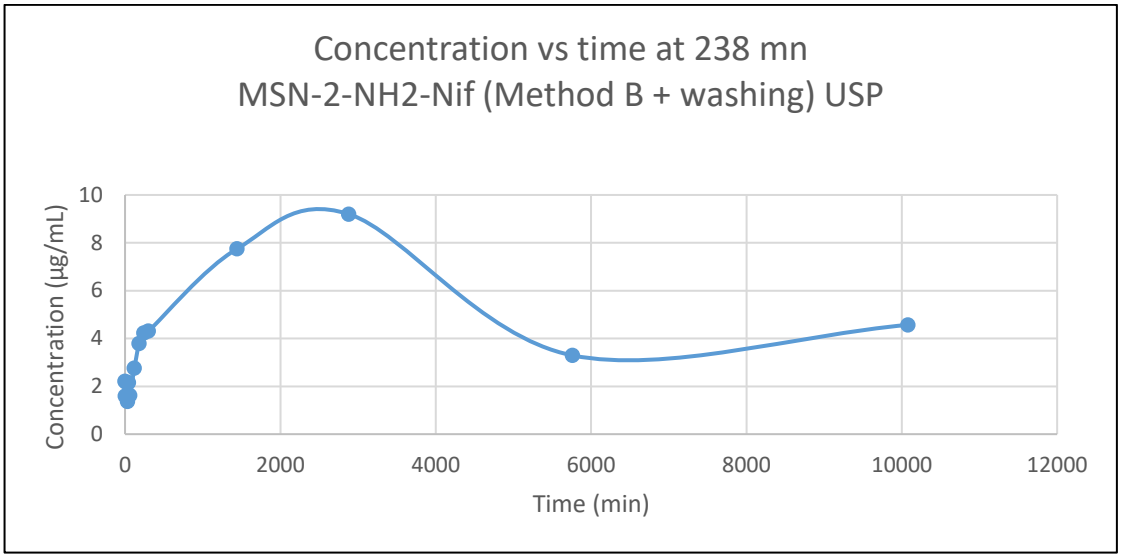

Figure 50 Evolution of the concentration with time for the USP release study.

The concentration of nifedipine increases until 2880 minutes and then decreases. As there is an increase of the nifedipine concentration in the release medium, it can be said that there is a release.

The highest concentration attained by the nifedipine is 9.20 µg/mL.

Tubes release

Here are the results of the release of nanoparticles introduced in falcon tubes. This was done with the Method B + washing (Figure 51) and Method A + washing (Figure 52). The nanoparticles were used in powder form.

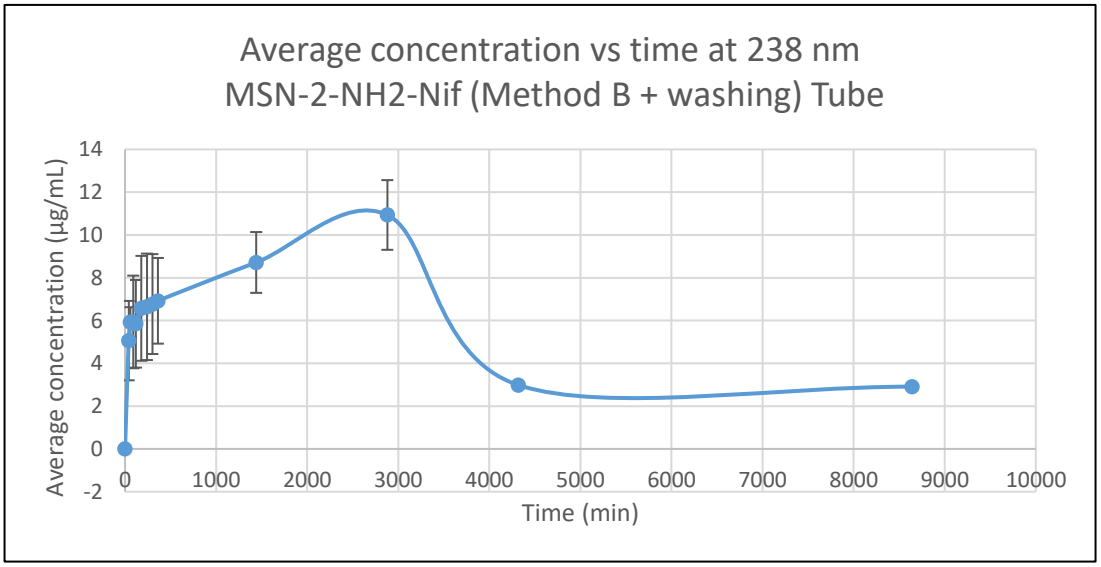

Figure 51 Evolution of the concentration with time for the Tube release study.

The concentration of nifedipine, in the release medium, increases rapidly until 120 minutes and then increases more slowly until 2880 minutes to finally decrease.

The higher concentration of the released nifedipine is 10.94 µg/mL.

The concentration of nifedipine increases more rapidly than with the dialysis and the USP. It can be due to the higher agitation (magnetic agitation for the tubes, rotation of the basket for the USP apparatus and magnetic agitation in the beaker where the membrane is immersed) in the tubes which provokes a faster release. And the drug has only one barrier, the nanoparticle.

It is possible to compare this results with those from the USP because the same sample is used. In both cases there is a release but the highest concentration for the USP is 9.20 µg/mL whereas for the tubes it is 10.94 µg/mL.

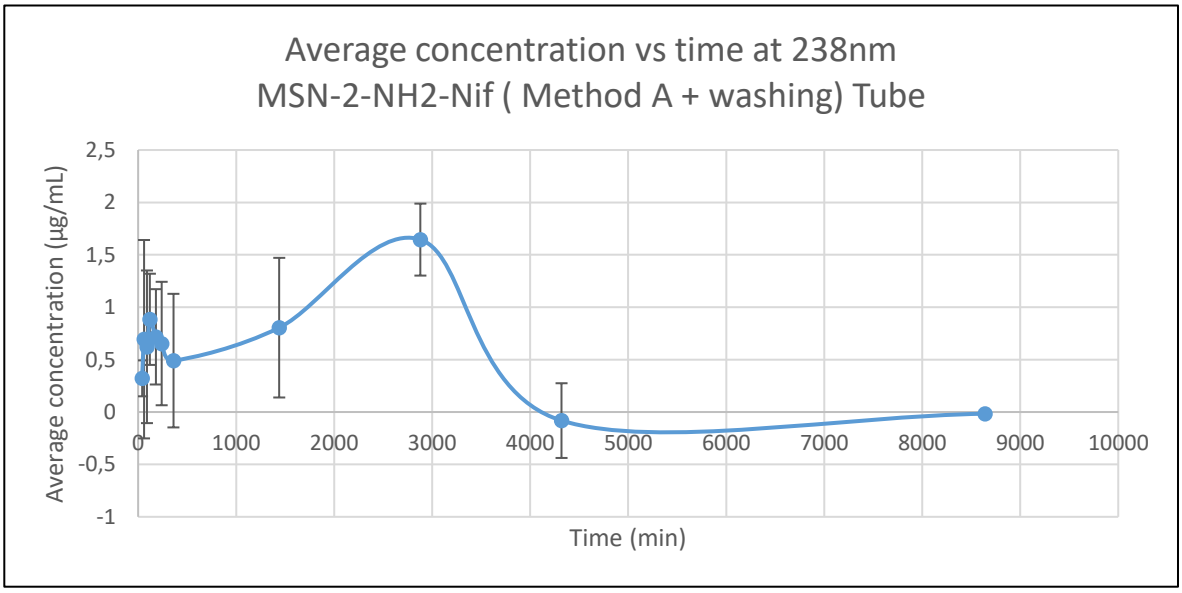

Figure 52 Evolution of the concentration with time for the Tube release study.

The concentration of nifedipine, in the release media, increases rapidly until 120 minutes. After this time, a decrease is monitoring following by an increase until 2880 minutes. After that the concentration decreases.

The highest value of concentration attained is 1.64 µg/mL.

Baseline test

A baseline test has been achieved to check the time stability and reproducibility (Figure 53). The cuvette was filled with PBS and one measurement was done each hour for 14 hours.

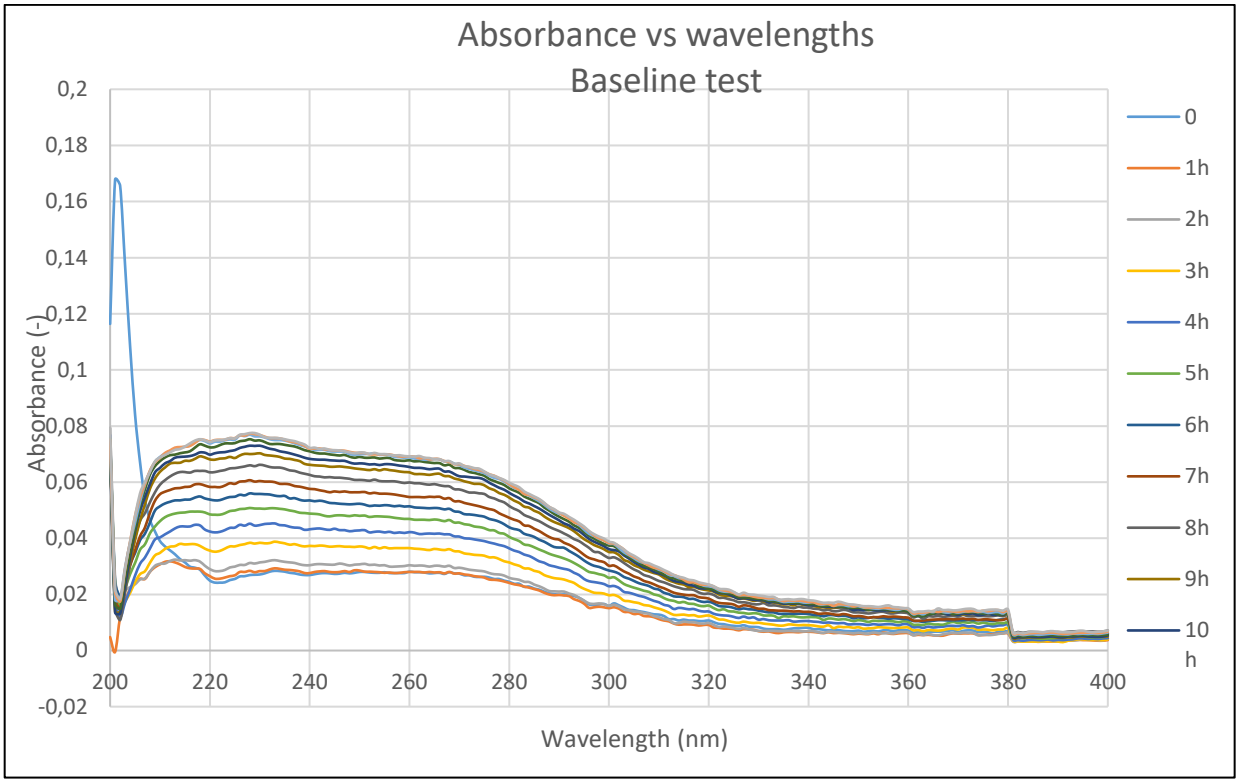

Figure 53 Evolution of the absorbance with the wavelengths for the baseline test.

The absorbance is not equal to zero with time, so the baseline is not stable. On the figure 53, the absorbance is gradually increasing with time. The first measurements are quite similar, then absorbance increases and stabilizes for the lasts ones.

Normally, the baseline measurements should be the same. One hypothesis is an energy change of the lamp between each measurement. It is possible that the lamp does not emit with the same energy (and the same intensity) during the whole experiment. As the absorbance depends on the intensity emitted by the lamp, it can result in fluctuations of the baseline.

This behavior of the baseline can explain some high error bars in the release results. It could also explain the difference between the concentration from the USP and the tube for the Method B + washing.

5. Conclusion

The synthesis of nanoparticles with 2 mL of APTES have been achieved. They have been loaded following different methods: Method B, Method B + washing, Method A + washing and Method C + washing. In these different methods, the number of rotary evaporation sessions varied as well as the washing of the loaded nanoparticles.

Afterwards the release of these nanoparticles from the different methods have been studied using the dialysis, the USP apparatus and falcon tubes. The results of these three methods have been compared to choose one of the method (table 4).

Table 4 Summary table of the project.

	Rotary evaporator	Washing	TGA	Release concentration
Method B	2	No	26.86%	8.15 mg/L (Dialysis)
Method B + washing	2	Yes	21.28%	9.20 mg/L (USP) 10.94 mg/L (Tube)
Method A + washing	0	Yes	2.97%	1.64 mg/L (Tube)
Method C + washing	1	Yes	3.12%	x

The method B shows the higher amount of nifedipine (26.86%) with 2 sessions of evaporation and no washing.
When washing is added (Method B + washing), the amount of nifedipine is a bit decreased (21.28%), possibly because of the removal of the nifedipine which is not on the surface of the nanoparticles or in the pores.
When there is no evaporation and only a removal of the supernatant (Method A + washing) the quantity of nifedipine is dramatically decreased (to 2.97%), possibly because of the lack of the evaporation which enhance the loading.
And when an evaporation is added to the process (Method C + washing), the amount of nifedipine is a little higher than in the Method A + washing.

The better solution for the loading is the Method B + washing. In this process the loaded is enhanced thanks to the 2 sessions of evaporation and the residual nifedipine is removed by the washing.

For the release, the Method B attains 8.15 mg/L which is few comparing with the initial concentration in the membrane. A possible explanation is that the membrane is not adapted to the drug and retains it.

Concerning the Method B + washing, the higher concentration reached during the USP experiment is 9.20 mg/L whereas with the tubes it is 10.94 mg/L. The concentrations are in the same range and the slight difference can be explain with the baseline test. As the baseline seems to change in a small range of absorbance, the results of the release study can be affected by small fluctuations. Another explication which should be taken into account is the form of the nanoparticles in each experiment. In the USP experiment, a pellet is done and the nanoparticles are compacted whereas with the tubes, they are in powder-form. In the pellet, it can be more difficult for the drug to be released.

With the Method A, the higher concentration obtained is 1.64 mg/L. The value is smaller than in the other release studies. But this is relevant regarding the TGA results.

Finally, the dialysis is excluded since it may retain the drug.
The results from the Method B + washing show comparable results between the USP and the tube. The tubes are the privilege solution because they are more easily used and less expensive than the USP apparatus.

By taking into consideration the results of the loading the Method B + washing is taken on. And regarding the results of the release experiments the best solution is to use tubes.

6. Further work

To follow this project, the next step which could be planned is the study of nifedipine loading and release from nanoparticles attached to titanium. The way to bind nanoparticles to titanium will not be explained here (see TFM Paul Game, 2017).

Loading

The sample will be received already covered with nanoparticles. It will be plunged in a solution of anhydrous methanol and nifedipine. For the loading of nanoparticles, a solution at 4 µg/mL was used for 160 mg of nanoparticles. In the case of the titanium samples, the nifedipine concentration can be lowered because the nanoparticles concentration will be lower.
The mixture will be kept under orbital agitation for 24 hours in a cold-water bath and covered with Aluminum foil to prevent the photodegradation of the nifedipine.

Considering the results of this project, it could be better to evaporate the methanol with the rotary evaporator. But, the stability of the sample (the sample must not turn over) in the flask must be certain not to alter the coating, as well as the thermal stability of the coating.

After the loading, the sample can be washed with a quick immersion in fresh anhydrous methanol and dried with nitrogen.

A possible way to characterize the loading could be to do an infrared spectrum of the sample via an ATR measurement.

Release

The release of the nifedipine will be done in adjusted PBS.
The sample can be plunged in a beaker with adjusted PBS and under orbital agitation. It must be protected from the light. The use of the USP apparatus can be considered because it allows the agitation and the heating of the medium at the same time.

For the characterization, the use of HPLC could be considered as the concentration of nifedipine may be low. However, the use of the UV-vis spectroscopy remains possible if the release medium volume is not too high (prevention of a too high dilution of the nifedipine whose concentration could be difficult to measure).
Nevertheless, independently of the method (HPLC or UV-vis spectroscopy) chosen, the concentration measurement should be done directly after having taken the aliquot.

7. Economic analysis

Table 1 Costs associated to the synthesis of nanoparticles.

Material	Quantity	Price	Cost (€)
NaOH	8 g	16.30€/kg	0.13
Distilled water	3.84 L	0.08€/L	0.31
CTAB	8 g	302.10€/g	2416.8
TEOS	36 mL	74.80€/L	2692.8
APTES	9 mL	53.50€/ 100mL	4.82
Total cost associated to the synthesis of nanoparticles			**5122.06**

Table 2 Costs associated to the purification of nanoparticles.

Material and equipment	Quantity	Price	Cost (€)
Distilled water	1 L	0.08€/L	0.08
Ethanol	1 L	25.50€/L	25.5
Methanol	1.5 L	31.75€/L	47.62
Ammonium nitrite	15 g	87.5 €/kg	1.31
Total cost associated to the purification of nanoparticles			**74.51**

Table 3 Costs associated to the loading of nanoparticles.

Material and equipment	Quantity	Price	Cost (€)
Nifedipine	0.6 g	54.00€/g	32.4
Anhydrous methanol	200 mL	59€/L	11.8
Freeze dryer	10	5€ / sample	50
Total cost associated to the loading of nanoparticles			**94.2**

Table 4 Costs associated to the release of nanoparticles.

Material and equipment	Quantity	Price	Cost (€)
PBS	5 L	30€/500mL	300
Dialysis membranes	2	113€/ 10 cassettes	22.6
USP apparatus	1	200€/ essay	200
Total cost associated to the release of nanoparticles			**522.6**

Table 5 Costs associated to the characterization of nanoparticles.

Equipment	Quantity	Price	Cost (€)
UV-vis spectroscopy	15 h	4.85€/h	72.75
FTIR	5 h	5.14€/h	25.7
TGA	6	60€/sample	360
Total cost associated to the characterization of nanoparticles			**458.45**

Table 6 Costs associated to human resources and others.

Resources	Hours	Price	Cost (€)
PhD	60	60€/h	3600
PhD student	100	30€/h	3000
Project student	400	20€/h	8000
Others (gloves, pipettes, boxes…)			250
Total cost associated to human resources and others			**14850**

To sum up, the total price of the project is about 21121€.

8. Environmental impact

The environmental impact has been considering during all steps of this project. The reactants were used in small quantities to prevent waste.

All the wastes are treated differently regarding their nature. There are different trashes for the solvents used (acids, bases, polar, non-polar). For specific chemical wastes, containers are provided to the laboratory personal. The name of the waste is written on the container and is treated apart from others. The identification and the follow-up of chemical wastes are very important. Once the containers are full, they are stored in a cabinet.

There are also different trashes for the solid wastes (non-contaminated wastes and contaminated ones). Selective sorting is also done in the laboratory. There are different trashes for paper, plastics and residues.

9. Annexes

9.1. Annex A

The following table gives a recap of the different USP apparatus. [37]

Name	Rotation speed	Medium volume	Used for
Apparatus I Rotating basket 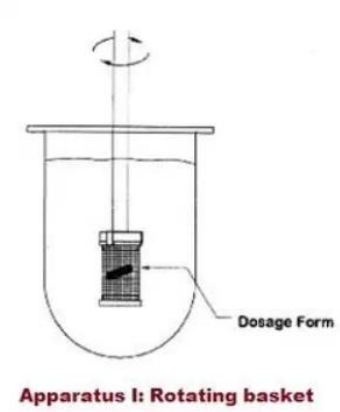	50-120 rpm	500-4000 mL	• Immediate release. • Delayed release. • Chewable tablets. • Extended release tablets and floating dosage form.
Apparatus II Paddle 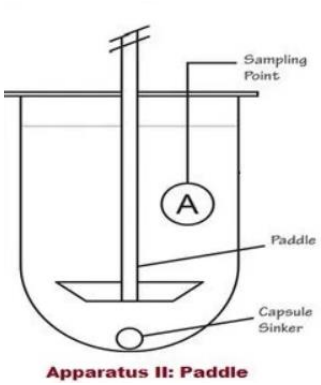	25-50 rpm	500-4000 mL	• Immediate release. • Orally disintegrating tablets. • Chewable tablets. • Delayed release. • Extended release tablets, capsules and suspension.

Apparatus III Reciprocating cylinder 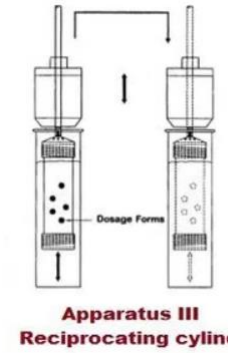 **Apparatus III Reciprocating cylinder**	6-35 rpm	250 mL	• Controlled release formulations • Chewable tablets.
Apparatus IV Flow through cell 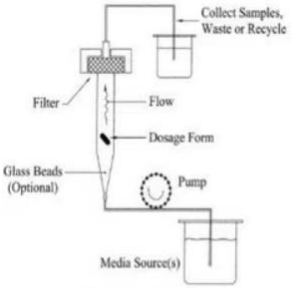 **Apparatus IV: Flow through cell**		Up to 3L per hour	• Drug product containing poorly soluble API. • Powder and granules. • Microparticles.
Apparatus V Paddle over disk 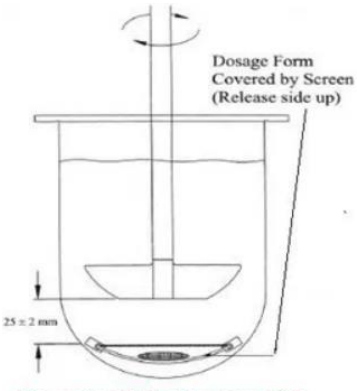 **Apparatus V: Paddle over disk**	25-50 rpm	500-4000 mL	• Transdermal patches. • Ointment. • Floaters and emulsions.

Apparatus VI Rotating cylinder 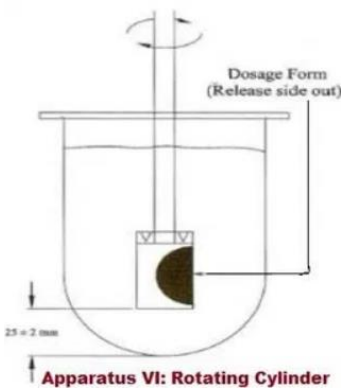	25-50 rpm	500-4000 mL	• Transdermal patches.
Apparatus VII Reciprocating holder 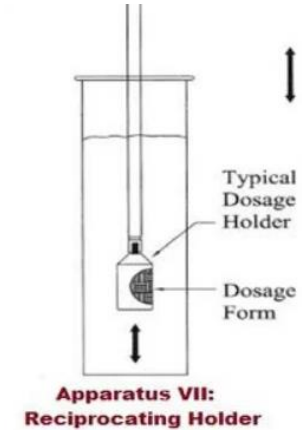	30 rpm	Variable	• Controlled release profile (transdermal formulations and non-disintegrating oral formulations). • pH profile.

9.2. Annex B

Here is the table used to analyze the infrared spectra (figure 54).

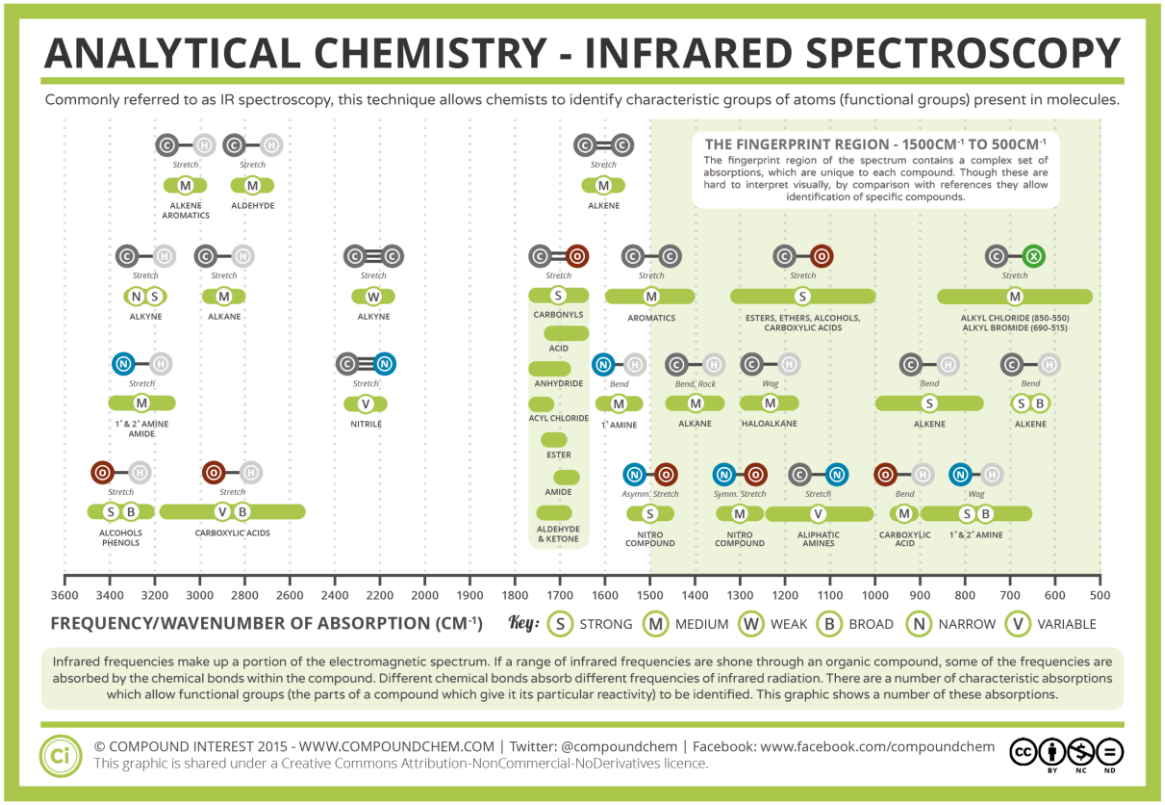

Figure 54 Infrared spectroscopy table [38].

9.3. Annex C

Here are the detailed calculations which have been done to calculate the loading percentage of nifedipine in the nanoparticles.

$$Nifedipine\ loading = \frac{\%\ mass\ loss\ loaded\ samples - \%\ mass\ loss\ empty\ samples}{\%\ mass\ loss\ pure\ drug} * 100$$

- Nifedipine
  % mass loss = 100.09 - 5.48= 94.61 %

- MSN-2-NH2
  % mass loss = 92.83 – 76.05 = 16.78 %

- MSN-2-NH2-Nif Method B
  % mass loss = 96.23 - 54.03 = 42.20 %

- MSN-2-NH2-Nif Method B + washing
  % mass loss = 97.89 – 60.98 = 36.91%

- MSN-2-NH2-Nif Method A + washing
  % mass loss = 96.67 – 77.08 = 19.59%

- MSN-2-NH2-Nif Method C + washing
  %mass loss = 96.56 -76.83 = 19.73%

Nifedipine loading:

- MSN-2-NH2-Nif Method B

$$\frac{42.2 - 16.78}{94.61} * 100 = 26.86\ \%$$

- MSN-2-NH2-Nif Method B + washing

$$\frac{36.91 - 16.78}{94.61} * 100 = 21.27\ \%$$

- MSN-2-NH2-Nif Method A + washing

$$\frac{19.59 - 16.78}{94.61} * 100 = 2.97\ \%$$

- MSN-2-NH2-Nif Method C + washing

$$\frac{19.73 - 16.78}{94.61} = 3.12\ \%$$

10. Bibliography

[1] R. P. Robertson and J. S. Harmon, "Diabetes, glucose toxicity, and oxidative stress: A case of double jeopardy for the pancreatic islet β cell," *Free Radic. Biol. Med.*, vol. 41, no. 2, pp. 177–184, 2006.

[2] OMS, "Rapport mondial sur le diabète 2013," p. 4, 2013.

[3] Docteur clic un service santé assistance, santé au quotidien, Diabète non insulino-dépendant, diabète de type 2 ou DNID https://www.docteurclic.com

[4] L. Piconi *et al.*, "Constant and intermittent high glucose enhances endothelial cell apoptosis through mitochondrial superoxide overproduction," *Diabetes. Metab. Res. Rev.*, vol. 22, no. 3, pp. 198–203, 2006.

[5] A. P. Robertson, "Chronic oxidative stress as a central mechanism for glucose toxicity in pancreatic islet beta cells in diabetes," *J. Biol. Chem.*, vol. 279, no. 41, pp. 42351–42354, 2004.

[6] P. Held, "An Introduction to Reactive Oxygen Species Measurement of ROS in Cells," *BioTek Instruments*, pp. 1–14, 2012.

[7] D. Munro"Production des espèces réactives de l'oxygène et composition lipidique des membranes motichondriales comme déterminant de la longévité et de la capacité d'adaptation au froid chez les bivalves vénéroïdes"octobre 2014.

[8] R. Mittler, "ROS Are Good," *Trends Plant Sci.*, vol. 22, no. 1, pp. 11–19, 2017.

[9] C. a S. Number, N. P. Description, and T. Uv, "Page 1 of 3," *Solutions*, pp. 9–11.

[10] I. J. Marques, P. D. Vaz, A. C. Fernandes, and C. D. Nunes, "Advantageous delivery of nifedipine from inorganic materials showing increased solubility and biocompatibility," Microporous Mesoporous Mater., vol. 183, no. January 2016, pp. 192–200, 2014.

[11] PubChem Open chemistry database, Nifedipine https://pubchem.ncbi.nlm.nih.gov

[12] A. Profiles and O. F. Drug, "Nifedipine syed," vol. 18, 1989.

[13] J. N. Latosińska, M. Latosińska, J. Seliger, and V. Žagar, "An innovative method for the non-destructive identification of photodegradation products in solid state: 1H-14N NMR-NQR and DFT/QTAIM study of photodegradation of nifedipine (anti-hypertensive) to nitrosonifedipine (potential anti-oxidative)," *Eur. J. Pharm. Sci.*, vol. 47, no. 1, pp. 97–107, 2012.

[14] R. P. Mason, P. Marche, and T. H. Hintze, “Novel Vascular Biology of Third-Generation L-Type Calcium Channel Antagonists: Ancillary Actions of Amlodipine,” *Arterioscler. Thromb. Vasc. Biol.*, vol. 23, no. 12, pp. 2155–2163, 2003.

[15] W. M. Yousef, A. H. Omar, M. D. Morsy, M. M. Abd El-Wahed, and N. M. Ghanayem, “The mechanism of action of calcium channel blockers in the treatment of diabetic nephropathy,” *Int J Diabetes Metab.*, vol. 13, pp. 76–82, 2005. A. Profiles and O. F. Drug, “Nifedipine syed,” vol. 18, 1989.

[16] I. T. Mak and W. B. Weglicki, “Comparative antioxidant activities of propranolol, nifedipine, verapamil, and diltiazem against sarcolemmal membrane lipid peroxidation,” *Circ. Res.*, vol. 66, no. 5, pp. 1449–1452, 1990.

[17] I. T. Mak, P. Boehme, and W. B. Weglicki, “Antioxidant effects of calcium channel blockers against free radical injury in endothelial cells,” *Circ. Res.*, vol. 70, pp. 1099–1103, 1992.

[18] R. Berkels, G. Egink, T. A. Marsen, H. Bartels, R. Roesen, and W. Klaus, “Nifedipine Increases Endothelial Nitric Oxide Bioavailability by Antioxidative Mechanisms,” *Hypertension*, vol. 37, no. 2, pp. 240–245, 2001.

[19] Y. Fukuhara *et al.*, “Protective effect of photodegradation product of nifedipine against tumor necrosis factor alpha-induced oxidative stress in human glomerular endothelial cells.,” *J. Med. Invest.*, vol. 58, no. 1–2, pp. 118–126, 2011.

[20] K. Tsukuda *et al.*, “Diabetes-associated cognitive impairment is improved by a calcium channel blocker, nifedipine,” *Hypertension*, vol. 51, no. 2 PART 2, pp. 528–533, 2008.

[21] A. Kiwilsza *et al.*, “Mesoporous drug carrier systems for enhanced delivery rate of poorly water-soluble drug: nimodipine,” *J. Porous Mater.*, vol. 22, no. 3, pp. 817–829, 2015.

[22] K. Nidhi, S. Indrajeet, M. Khushboo, K. Gauri, and D. J. Sen, “Hydrotropy: A promising tool for solubility enhancement: A review,” *Int. J. Drug Dev. Res.*, vol. 3, no. 2, pp. 26–33, 2011.

[23] A. Kiwilsza *et al.*, “Molecular dynamics and the dissolution rate of nifedipine encapsulated in mesoporous silica,” *Microporous Mesoporous Mater.*, vol. 250, pp. 186–194, 2017.

[24] A. Szegedi, M. Popova, I. Goshev, S. Klébert, and J. Mihály, “Controlled drug release on amine functionalized spherical MCM-41,” *J. Solid State Chem.*, vol. 194, no. July 2015, pp. 257–263, 2012.

[25] D. Ghosh, A. K. Pradhan, S. Mondal, N. A. Begum, and D. Mandal, “Proton transfer reactions of 4’-chloro substituted 3-hydroxyflavone in solvents and aqueous micelle

solutions," *Phys. Chem. Chem. Phys.*, vol. 16, no. 18, p. 8594, 2014.

[26] E. Lafontaine, "Microémulsions Solidifées : Une nouvelle voie pour les conducteurs protoniques ?," 2014.

[27] I. A. Rahman and V. Padavettan, "Synthesis of Silica nanoparticles by Sol-Gel: Size-dependent properties, surface modification, and applications in silica-polymer nanocompositesa review," *J. Nanomater.*, vol. 2012, 2012.

[28] MCL materials and chemistry laboratory, 3D Networks of Mesoporous Silica Nanoparticles www.matchemlab.com

[29] N. H. N. Kamarudin *et al.*, "Role of 3-aminopropyltriethoxysilane in the preparation of mesoporous silica nanoparticles for ibuprofen delivery: Effect on physicochemical properties," *Microporous Mesoporous Mater.*, vol. 180, pp. 235–241, 2013.

[30] R. Yadollahi, K. Vasilev, C. A. Prestidge, and S. Simovic, "Polymeric nanosuspensions for enhanced dissolution of water insoluble drugs," *J. Nanomater.*, vol. 2013, 2013.

[31] S. Dru *et al.*, "Efficient Loading and Encapsulation of Anti- Tuberculosis Drugs using Multifunctional Mesoporous Silicate Nanoparticles ,"journal of nanosciences: current research, vol.1, 2016.

[32] Appplidyne Engineering Desing, FTIR Spectrometer Vibration Investigation https://www.applidyne.com

[33] SlideShare Thermal Analysis Terry A. Ring Chemical Engineering University of Utah https://www.slideshare.net

[34] P. Breuil and G. Bouchoux, "Spectrophotométrie d' absorption dans l' ultraviolet et le visible," *Tech. l'ingénieur*, vol. 33, no. 0, p. 20, 2014.

[35] Operation guide UV-1800 Shimadzu Spectrophotometer, Shimadzu Coorperation, 2008

[36] A. C. S. A. Materials, "Cu and Zr modified SBA-15 as drug carriers for dental appli-cations : synthesis , loading , and release."

[37] Pharmalearners, Types of Dissolution Apparatus and their Applications as Per USP http://www.pharmalearners.com

[38] Compound interest, Analytical Chemistry-Infrared Spectroscopy www.compoundchem.com

[39] C. Degletagne and D. Cyril, “Penguin acclimatization to polar environmental constraints : a transcriptomic and integrative study in King ...,” no. February, 2016.

[40] F. Wauquier, L. Leotoing, V. Coxam, J. Guicheux, and Y. Wittrant, “Oxidative stress in bone remodelling and disease,” *Trends Mol. Med.*, vol. 15, no. 10, pp. 468–477, 2009.

[41] Y. Hamada, H. Fujii, and M. Fukagawa, “Role of oxidative stress in diabetic bone disorder,” *Bone*, vol. 45, no. SUPPL. 1, pp. S35–S38, 2009.

[42] Lang, N., & Tuel, A. (2004). A fast and efficient ion-exchange procedure to remove surfactant molecules from MCM-41 materials. Chemistry of Materials, 16(10), 1961–1966. https://doi.org/10.1021/cm030633n

[43] Rad, B. A., Tarlani, A., Jameh-Bozorghi, S., & Niazi, A. (2017). Facile, low-cost, and organic-free fabrication of diverse nanoporous alumina as support for drug release; on the salt effect, calcination temperature, and reaction time dependence. Journal of Sol-Gel Science and Technology, 83(3), 627–639. https://doi.org/10.1007/s10971-017-4454-4